On the dynamical influence of ocean eddy potential vorticity fluxes

Ocean Modelling 92 (2015) 169–182

Contents lists available at ScienceDirect

Ocean Modelling

journal homepage: www.elsevier.com/locate/ocemod

On the dynamical influence of ocean eddy potential vorticity fluxes

J.R. Maddison [a,*], D.P. Marshall [b], J. Shipton [c]

[a] School of Mathematics and Maxwell Institute for Mathematical Sciences, University of Edinburgh, Edinburgh, EH9 3FD, United Kingdom
[b] Department of Physics, University of Oxford, Oxford, OX1 3PU, United Kingdom
[c] Department of Mathematics, Imperial College London, London, SW7 2AZ, United Kingdom

ARTICLE INFO

Article history:
Received 27 January 2015
Revised 2 June 2015
Accepted 13 June 2015
Available online 19 June 2015

Keywords:
Ocean eddy fluxes
Helmholtz decomposition
Potential vorticity
Eddy force
Dynamics

ABSTRACT

The impact of eddy potential vorticity fluxes on the dynamical evolution of the flow is obscured by the presence of large and dynamically-inert rotational fluxes. However, the decomposition of eddy potential vorticity fluxes into rotational and divergent components is non-unique in a bounded domain and requires the imposition of an additional boundary condition. Here it is proposed to invoke a one-to-one correspondence between divergent eddy potential vorticity fluxes and non-divergent eddy momentum tendencies in the quasi-geostrophic residual-mean equations in order to select a unique divergent eddy potential vorticity flux. The divergent eddy potential vorticity flux satisfies a zero tangential component boundary condition. In a simply connected domain, the resulting divergent eddy potential vorticity flux satisfies a powerful optimality condition: it is the horizontally oriented divergent flux with minimum L^2 norm. Hence there is a well-defined sense in which this approach removes as much of the dynamically inactive eddy potential vorticity flux as possible, and extracts an underlying dynamically active divergent eddy potential vorticity flux. It is shown that this approach leads to a divergent eddy potential vorticity flux which has an intuitive physical interpretation, via a direct relationship to the resulting forcing of the mean circulation.

1. Introduction

The fundamental dynamical equations for the ocean can typically be cast into a flux form in which changes to physical quantities depend upon the divergence of their flux. This reflects the existence of integral conservation laws and yields a natural physical interpretation in terms of the transport of properties such as heat, salinity, or potential vorticity from one region of the ocean to another. However, in practice, the direct analysis of the dynamical impact of oceanic fluxes is often obscured by the existence of large *non-divergent* flux components, which necessarily have no direct dynamical effect. The general resolution of this issue is through the application a Helmholtz decomposition, separating the flux into a divergent component, which is dynamically active, and a non-divergent component, which is dynamically inert. Unfortunately, this decomposition is inherently non-unique in bounded domains, and is dependent upon a choice of boundary conditions (Fox-Kemper et al., 2003).

This issue is of particular concern in the analysis and comparison of eddy parameterisations, which typically specify parameterised eddy fluxes. For example, the existence of locally up-gradient fluxes does not necessarily rule out the application of down-gradient flux parameterisations – an appropriately defined divergent eddy flux may be more closely aligned counter to the mean gradients (e.g. Marshall and Shutts, 1981). Similarly, down-gradient potential vorticity closures violate momentum conservation constraints in general (Bretherton, 1966; Marshall et al., 2012), but momentum conservation can be restored via the introduction of an appropriate non-divergent eddy potential vorticity flux (Eden, 2010).

In a domain average sense, eddy potential vorticity fluxes must be oriented down the mean gradient in order to ensure net generation of eddy enstrophy, itself required in order to balance small-scale enstrophy dissipation. However it has long been recognised that this principle need not hold locally (Harrison, 1978; Holland and Rhines, 1980). Local fluxes of eddy enstrophy permit the eddy potential vorticity flux to be oriented in any direction. In Marshall and Shutts (1981) eddy fluxes are separated into a component balancing the mean advection and a residual component. In the barotropic vorticity model of Marshall (1984) it is found that the residual eddy potential vorticity flux thus defined is more strongly aligned with the mean potential vorticity gradient. The methodology is directly generalised in Nakamura (1998) and Nakamura and Chao (2002). A related approach is described in Greatbatch (2001) and Medvedev and Greatbatch (2004), whereby the eddy fluxes are separated into advective, diffusive, and rotational fluxes, which are then related to the

* Corresponding author. Tel.: +44 131 6505036.
E-mail address: j.r.maddison@ed.ac.uk (J.R. Maddison).

http://dx.doi.org/10.1016/j.ocemod.2015.06.003

components of the total (mean plus eddy) advective eddy variance flux in the along and across mean gradient directions. This results in a decomposition similar to the Temporal Residual Mean I formulation of McDougall and McIntosh (1996) (with the latter replacing the use of the total advective eddy variance flux with the mean advective eddy variance flux – see Maddison and Marshall (2013, Appendix B) for further details). The decomposition of Medvedev and Greatbatch (2004) is itself generalised in Eden et al. (2007) via the consideration of higher order eddy budgets.

An alternative approach is to decompose eddy potential vorticity fluxes into rotational and divergent components via the use of a Helmholtz decomposition (e.g. Lau and Wallace, 1979). In Roberts and Marshall (2000) ocean eddy fluxes, diagnosed from a primitive equation model, are decomposed into rotational and divergent components via the application of a Helmholtz decomposition, subject to zero normal divergent flux boundary conditions. The resulting divergent eddy fluxes are in this case found to be rather poorly correlated with corresponding mean gradients.

Non-uniquness of the Helmholtz decomposition in bounded domains, and consequences for the decomposition of eddy fluxes, is discussed at length in Fox-Kemper et al. (2003). The zero normal divergent flux boundary condition is only one of countless valid options. Subject to an alternative choice of boundary conditions it is possible, in a bounded domain, to extract an eddy flux which has a minimum norm, or a minimum deviation from the mean gradient (Fox-Kemper et al., 2003). Without any additional constraints on the problem there is no way to select a boundary condition from amongst these options.

This article discusses a physically motivated approach for resolving this ambiguity in the Helmholtz decomposition of eddy potential vorticity fluxes. Specifically the quasi-geostrophic residual-mean equations allow the identification of a one-to-one correspondence between divergent eddy potential vorticity fluxes and non-divergent eddy momentum tendencies. The definition of the latter leads to an unambiguous definition of the former, which leads to a unique divergent eddy potential vorticity flux which satisfies a zero tangential component boundary condition. In a simply connected domain the resulting divergent eddy potential vorticity flux satisfies a powerful optimality condition: it is the (horizontally oriented) divergent flux with minimum L^2 norm. Hence there is a well-defined sense in which this approach removes as much of the dynamically inactive non-divergent eddy potential vorticity flux as possible, and extracts an underlying dynamically active divergent eddy potential vorticity flux. It is shown that this approach leads to a divergent eddy potential vorticity flux which has an intuitive physical interpretation, via a direct relationship to the resulting forcing of the mean circulation.

The paper proceeds as follows. Section 2 describes the mathematical formulation. The quasi-geostrophic residual-mean equations are outlined, and the relationship between divergent potential vorticity fluxes and non-divergent momentum tendencies is described. A stream function tendency, or "force function", is used to define the divergent potential vorticity fluxes, and it is shown that in a simply connected domain the resulting divergent potential vorticity flux satisfies an optimality property. Resulting divergent eddy potential vorticity fluxes are diagnosed from a three layer quasi-geostrophic model in Section 3. The decomposition is compared against the more conventional use of zero normal divergent potential vorticity flux boundary conditions, and the utility for the assessment of eddy parameterisations is considered. The paper concludes in Section 4.

2. Formulation

This section describes the Helmholtz decomposition of arbitrary potential vorticity fluxes into divergent and non-divergent components. Section 2.1 describes the horizontal Helmholtz decomposition, and discusses the origin of ambiguity in decomposing vector fields into divergent and rotational components. Section 2.2 introduces the quasi-geostrophic residual-mean equations, and uses these to the relate divergent potential vorticity fluxes to non-divergent momentum tendencies. In Section 2.3 this relation is used to define a horizontal Helmholtz decomposition for potential vorticity fluxes, by relating the divergent component of potential vorticity fluxes to stream function tendencies, or "force functions", associated with momentum tendencies. The assertion that the decomposition should be linear defines a unique horizontal Helmholtz decomposition for the eddy potential vorticity flux. Finally in Section 2.4 it is shown that, in a simply connected domain, the resulting divergent eddy potential vorticity flux is optimal, in that it is the unique (horizontally aligned) divergent eddy potential vorticity flux with minimal L^2 norm. The resulting diagnostic equations for force functions are summarised in Section 2.5.

2.1. Horizontal Helmholtz decomposition

The Helmholtz decomposition of a vector field splits the field into three components: a divergent component (with zero curl), a rotational component (with zero divergence), and a harmonic component (with both zero curl and zero divergence). This article considers the horizontal Helmholtz decomposition which, for a vector field $\mathbf{F}$, takes the form:

$$\mathbf{F} = \nabla_H \Phi_F + \hat{\mathbf{z}} \times \nabla_H \Psi_F + \mathbf{H}_F, \tag{1}$$

where Φ_F and Ψ_F are two scalar potentials, the divergent component is $\nabla_H \Phi_F$, the rotational component is[1] $\hat{\mathbf{z}} \times \nabla_H \Psi_F$, and the harmonic component is $\mathbf{H}_F$. $\mathbf{H}_F$ has both zero divergence and zero horizontal curl, $\nabla_H \cdot \mathbf{H}_F = (\hat{\mathbf{z}} \times \nabla_H) \cdot \mathbf{H}_F = 0$. $\nabla_H = (\partial_x, \partial_y, 0)^T$ is the horizontal gradient operator, and $(\hat{\mathbf{z}} \times \nabla_H) \cdot (\dots)$ is the horizontal curl operator.

A horizontal Helmholtz decomposition of $\mathbf{F}$ can in principle be performed by solving for the two potentials Φ_F and Ψ_F, and then using these to compute the harmonic residual $\mathbf{H}_F$. Taking the divergence and horizontal curl of $\mathbf{F}$ leads to two elliptic problems for the potentials:

$$\nabla_H^2 \Phi_F = \nabla_H \cdot \mathbf{F} \tag{2a}$$

$$\nabla_H^2 \Psi_F = (\hat{\mathbf{z}} \times \nabla_H) \cdot \mathbf{F}. \tag{2b}$$

The critical issue here is that no boundary conditions have been imposed on these problems. The selection of alternative boundary conditions allows harmonic fields to be exchanged between the divergent, rotational, and harmonic components of the decomposition. Without the specification of appropriate boundary conditions (e.g. as discussed in Denaro (2003)) the Helmholtz decomposition of a vector field is, in a bounded domain, not unique.

2.2. The quasi-geostrophic residual-mean equations

We now explicitly limit consideration to the quasi-geostrophic equations. A quantity θ is decomposed into a mean component $\overline{\theta}$ and an eddy component $\theta' = \theta - \overline{\theta}$.[2] The mean quasi-geostrophic momentum and buoyancy equations are then:

$$\begin{aligned}\partial_t \overline{\mathbf{u}_g} + \overline{\mathbf{u}_g} \cdot \nabla_H \overline{\mathbf{u}_g} + f_0 \hat{\mathbf{z}} \times \overline{\mathbf{u}_{ag}} + \beta y \hat{\mathbf{z}} \times \overline{\mathbf{u}_g} \\ = -\frac{1}{\rho_0} \nabla_H \overline{p_{ag}} + \overline{\mathbf{S}} - \overline{\mathbf{u}_g' \cdot \nabla_H \mathbf{u}_g'},\end{aligned} \tag{3a}$$

$$\partial_t \overline{b} + \nabla_H \cdot \left(\overline{\mathbf{u}_g} \overline{b}\right) + \overline{w_{ag}} N_0^2 = \overline{B} - \nabla_H \cdot \overline{\mathbf{u}_g' b'}, \tag{3b}$$

where $\mathbf{u}_g$ is the geostrophic velocity, $\mathbf{u}_{ag}$ is the horizontal component of the ageostrophic velocity, and w_{ag} is the vertical component

[1] Here the horizontal skew-gradient is equivalent to a three-dimensional curl via $\hat{z} \times \nabla_H \Psi = -\nabla_H \times (\Psi \hat{\mathbf{z}}) = -\nabla \times (\Psi \hat{\mathbf{z}})$, where ∇ is the three-dimensional gradient operator.

[2] It is assumed that $\overline{(\dots)}$ is a linear projection operator which commutes with the $\hat{\mathbf{z}}\times$ operator and with derivatives with respect to space and time. It is further assumed that f_0, βy, ρ_0, and N_0 have zero eddy component.

of the ageostrophic velocity. In the quasi-geostrophic limit the mean geostrophic and ageostrophic velocities are each non-divergent:

$$\nabla_H \cdot \overline{\mathbf{u}_g} = \nabla_H \cdot \overline{\mathbf{u}_{ag}} + \partial_z \overline{w_{ag}} = 0. \tag{4}$$

p_{ag} is the ageostrophic pressure, b is the buoyancy, $f = f_0 + \beta y$ is the Coriolis parameter, ρ_0 is the reference density, N_0 is the buoyancy frequency, and $\mathbf{S} = (S_x, S_y, 0)^T$ and B include additional forcing and dissipation.

As is described below the quasi-geostrophic residual-mean equations are reached by noting that there is a dynamical equivalence between horizontal fluxes of buoyancy and vertical fluxes of momentum. This can be used to remove the eddy buoyancy flux from the buoyancy equation, subject to the addition of a compensating term in the momentum equation (Andrews and McIntyre, 1976; 1978; Nurser and Lee, 2004), (Marshall et al., 2012, appendix). See Maddison and Marshall (2013) for an overview of such transformations for the quasi-geostrophic equations.

Consider the following residual-mean ageostrophic velocity:

$$\mathbf{u}^*_{ag} + w^*_{ag}\hat{\mathbf{z}} = \overline{\mathbf{u}_{ag}} + \overline{w_{ag}}\hat{\mathbf{z}} + \frac{1}{f_0}\nabla \times \begin{pmatrix} \frac{f_0}{N_0^2}\overline{v_g b} \\ -\frac{f_0}{N_0^2}\overline{u_g b} \\ \frac{1}{2N_0^2}\overline{b^2} - \overline{u_g^2} - \overline{v_g^2} \end{pmatrix}.$$

where ∇ is the three-dimensional gradient operator. Substitution leads to:

$$\partial_t \overline{\mathbf{u}_g} + \hat{\mathbf{z}} \times \overline{\mathbf{u}_g} \overline{q} + f_0 \hat{\mathbf{z}} \times \mathbf{u}^*_{ag} = -\frac{1}{\rho_0}\nabla_H \overline{p_{ag}} + \overline{\mathbf{S}} - \hat{\mathbf{z}} \times \overline{\mathbf{u}'_g q'}, \tag{5a}$$

$$\partial_t \overline{b} + w^*_{ag} N_0^2 = \overline{B}, \tag{5b}$$

where q is the quasi-geostrophic potential vorticity (QGPV):

$$q = (\hat{\mathbf{z}} \times \nabla_H) \cdot \mathbf{u}_g + \beta y + \partial_z\left(\frac{f_0}{N_0^2} b\right). \tag{6}$$

No mean or eddy buoyancy fluxes appear in the residual-mean buoyancy Eq. (5b), and these are instead replaced by the appearance of mean and eddy potential vorticity fluxes in the residual-mean momentum Eq. (5a).

The residual-mean momentum Eq. (5a) can be expressed:

$$\partial_t \overline{\mathbf{u}_g} = -\hat{\mathbf{z}} \times \mathbf{F}, \tag{7}$$

with:

$$\mathbf{F} = \overline{\mathbf{u}_g} \overline{q} + \overline{\mathbf{u}'_g q'} + f_0 \mathbf{u}^*_{ag} - \frac{1}{\rho_0}\hat{\mathbf{z}} \times \nabla_H \overline{p_{ag}} + \hat{\mathbf{z}} \times \overline{\mathbf{S}}. \tag{8}$$

Since the mean geostrophic velocity is non-divergent it follows that:

$$\nabla_H \cdot (\partial_t \overline{\mathbf{u}_g}) = \nabla_H \cdot (-\hat{\mathbf{z}} \times \mathbf{F}) = 0, \tag{9}$$

and hence $-\hat{\mathbf{z}} \times \mathbf{F}$ is the non-divergent momentum tendency. The divergent component of momentum tendencies project onto the ageostrophic terms in the momentum equation, so that the total momentum tendency is horizontally non-divergent.

Taking the horizontal curl of Eq. (7), the z-derivative of Eq. (5b), and using (4), leads to the mean QGPV equation:

$$\partial_t \overline{q} = -\nabla_H \cdot (\mathbf{F} - f_0 \mathbf{u}^*_{ag}) + \partial_z\left(\frac{f_0}{N_0^2}\overline{B}\right). \tag{10}$$

Hence $\mathbf{F}$ can now be explicitly identified as a potential vorticity flux. Moreover its horizontal curl vanishes by Eq. (9):

$$(\hat{\mathbf{z}} \times \nabla_H) \cdot \mathbf{F} = \nabla_H \cdot (-\hat{\mathbf{z}} \times \mathbf{F}) = 0. \tag{11}$$

Hence the momentum equation defines the non-divergent momentum tendency, which then defines a *unique* horizontally curl free potential vorticity flux $\mathbf{F}$.

2.3. The force function and divergent potential vorticity fluxes

It is typical that, given a non-divergent velocity field, one introduce an appropriate corresponding stream function. For example, given the non-divergent mean geostrophic velocity $\overline{\mathbf{u}_g}$, the mean quasi-geostrophic stream function $\overline{\psi}$ is defined so that $\overline{\mathbf{u}_g} = \hat{\mathbf{z}} \times \nabla_H \overline{\psi}$. Marshall and Pillar (2011) extend this principle to momentum tendencies via the introduction of a corresponding *force* function.[3] For example, given the non-divergent mean geostrophic velocity tendency $\partial_t \overline{\mathbf{u}_g}$, a corresponding force function Ψ is defined so that $\partial_t \overline{\mathbf{u}_g} = \hat{\mathbf{z}} \times \nabla_H \Psi$. The mean stream function tendency and force function are thus equal up to an arbitrary function of z and t:

$$\Psi = \partial_t \overline{\psi} + c(z, t). \tag{12}$$

We now limit consideration to a simply connected domain with no-normal-flow boundary conditions for $\overline{\mathbf{u}_g}$, which leads to Dirichlet boundary conditions for $\overline{\psi}$. In this case it suffices to choose $c(z, t)$ such that $\Psi = 0$ on all lateral boundaries – that is homogeneous Dirichlet boundary conditions may be applied to the force function Ψ. Note that the quasi-geostrophic stream function defines both the horizontal momentum tendency and a buoyancy tendency, and hence the vertical derivative (which depends upon the values on the boundary) is of dynamical significance, and is set by mass and momentum constraints (McWilliams, 1977), (Pedlosky, 1987, section 3.25). The force function defines a horizontal momentum tendency only, and hence such constraints are not applied (that is, the $c(z, t)$ gauge vanishes under the horizontal gradient).

Substitution of the force function definition into Eq. (7) leads to:

$$\partial_t \overline{\mathbf{u}_g} = -\hat{\mathbf{z}} \times \mathbf{F} = \hat{\mathbf{z}} \times \nabla_H \Psi, \tag{13}$$

which defines a horizontal Helmholtz decomposition for the momentum tendency $-\hat{\mathbf{z}} \times \mathbf{F}$, with zero divergent and harmonic components. It immediately follows (by applying the $\hat{\mathbf{z}} \times (\dots)$ operator) that the corresponding potential vorticity flux has a horizontal Helmholtz decomposition:

$$\mathbf{F} = -\nabla_H \Psi, \tag{14}$$

and hence the potential vorticity flux $\mathbf{F}$ has zero rotational or harmonic component, and is uniquely defined in terms of the force function Ψ.

The force function defines a horizontal Helmholtz decomposition of the total momentum tendency $-\hat{\mathbf{z}} \times \mathbf{F}$, and equivalently of the potential vorticity flux $\mathbf{F}$. Since the eddy potential vorticity flux, $\overline{u'_g q'}$, is only one term in the full potential vorticity flux, a unique definition for the horizontal Helmholtz decomposition of an arbitrary potential vorticity flux is required. This is achieved by asserting that the force function for the sum of two momentum tendencies must equal the sum of their respective force functions. That is, a potential vorticity flux and its associated force function must be related via a linear operator or, equivalently, a potential vorticity flux and its divergent component must be related via a linear operator. This ensures that the elliptic problems for the force functions associated with differing momentum tendencies are decoupled.

More precisely, let the operator Π map an arbitrary momentum tendency $\mathbf{G}$ to its force function $\Psi_G = \Pi(\mathbf{G})$, where:

$$\mathbf{G} = \nabla_H \Phi_G + \hat{\mathbf{z}} \times \nabla_H \Psi_G + \mathbf{H}_G. \tag{15}$$

Then given two momentum tendencies $\mathbf{G}_1$ and $\mathbf{G}_2$ and arbitrary constants a_1 and a_2 linearity requires that:

$$\Pi(a_1 \mathbf{G}_1 + a_2 \mathbf{G}_2) = a_1 \Pi(\mathbf{G}_1) + a_2 \Pi(\mathbf{G}_2). \tag{16}$$

This linearity principle, combined with the use of homogeneous Dirichlet boundary conditions for the total force function Ψ, implies

[3] See also Lau and Wallace (1979), where the term "flux streamfunction" is used in the definition of rotational eddy fluxes.

that the force function for *any* momentum tendency is also subject to homogeneous Dirichlet boundary conditions. Moreover this implies that the divergent components of potential vorticity fluxes satisfy a zero tangential component boundary condition.

In particular, the horizontal Helmholtz decomposition for the eddy potential vorticity flux becomes:

$$\overline{\mathbf{u}_g' q'} = -\nabla_H \Psi_e + \hat{\mathbf{z}} \times \nabla_H \Phi_e + \hat{\mathbf{z}} \times \mathbf{H}_e \tag{17a}$$

and the eddy force function Ψ_e is then the solution of:

$$\nabla_H^2 \Psi_e = -\nabla_H \cdot \overline{\mathbf{u}_g' q'} \tag{18a}$$

$$\Psi_e = 0 \text{ on } \partial\Omega, \tag{18b}$$

where $\partial\Omega$ is the boundary of the horizontal domain Ω. The application of a horizontal Helmholtz decomposition, its relation to an eddy force function, and the assertion that the decomposition is linear, are sufficient to define a *unique* divergent eddy potential vorticity flux.

2.4. Optimality

The aim of performing a Helmholtz decomposition of the eddy potential vorticity flux is to remove a rotational and harmonic component, which may be large (Griesel et al., 2009; Jayne and Marotzke, 2002; Marshall and Shutts, 1981), so that an underlying dynamically active divergent component can be exposed. It is therefore meaningful to consider the Helmholtz decomposition which filters out as much of the eddy potential vorticity flux as possible – that is, the decomposition which yields the divergent component that is as small as possible. The eddy force function satisfies exactly this property in a simply connected domain. That is, among all scalar potentials which define a divergent component of the eddy potential vorticity flux, the force function yields the unique divergent flux $-\nabla_H \Psi_e$ whose L^2 norm $\sqrt{\int_\Omega \nabla_H \Psi_e \cdot \nabla_H \Psi_e}$ is minimised. See Appendix A for a proof of this property.

2.5. Diagnostic equations

In summary, writing the residual-mean momentum Eq. (5a) as:

$$\partial_t \overline{u}_g = \sum_i \mathbf{G}_i, \tag{19}$$

then in a simply connected domain the force function associated with an arbitrary momentum tendency $\mathbf{G}_i$ is defined via:

$$\nabla_H^2 \Psi_{G_i} = (\hat{\mathbf{z}} \times \nabla_H) \cdot \mathbf{G}_i, \tag{20a}$$

$$\Psi_{G_i} = 0 \text{ on } \partial\Omega, \tag{20b}$$

which defines a horizontally rotational component of the momentum tendency $\hat{\mathbf{z}} \times \nabla_H \Psi_{G_i}$. The eddy force function is then defined via (18), yielding a horizontally divergent comment of the eddy potential vorticity flux via (17).

For the quasi-geostrophic equations there is an equivalence between the vertical derivative of buoyancy tendencies (multiplied by f_0/N_0^2) and the horizontal curl of momentum tendencies. That is, any buoyancy tendency may be transformed into a horizontal momentum tendency (which is defined up to the addition of a horizontally non-divergent gauge). Hence if the mean QGPV Eq. (10) is written as:

$$\partial_t \overline{q} = \sum_i Q_i, \tag{21}$$

then a force function associated with each potential vorticity tendency Q_i can be defined via:

$$\nabla_H^2 \Psi_{Q_i} = Q_i \tag{22a}$$

$$\Psi_{Q_i} = 0 \text{ on } \partial\Omega. \tag{22b}$$

This, for example, allows for the calculation of a full force function budget, accounting for any residual arising from a non-zero $\partial_t \overline{q}$, and for terms defined directly in terms of a potential vorticity tendency (such as the wind forcing (26) in the numerical example to follow).

3. Numerical example

In this section eddy fluxes are diagnosed from a three layer quasi-geostrophic model. The eddy fluxes are decomposed using a horizontal Helmholtz decomposition, with the dynamically active divergent component defined using the eddy force function described in the previous section. The model equations and configuration are outlined in Section 3.1. The decomposition of mean potential vorticity fluxes is briefly described in Section 3.2. The decomposition of eddy fluxes is described in Section 3.3, and this is compared against a decomposition with zero normal divergent flux boundary conditions in Section 3.4. Finally the utility of the eddy force function for assessment of mesoscale eddy parameterisations is considered in Section 3.5, by considering a basic down-gradient potential vorticity parameterisation.

3.1. Multi-layer quasi-geostrophic model

The multi-layer quasi-geostrophic equations are (Pedlosky, 1987; Vallis, 2006):

$$\partial_t q_i + \nabla_H \cdot (\mathbf{u}_{g,i} q_i) = \nu \nabla_H^2 \omega_i - r \delta_{in} \omega_i + \delta_{i1} Q_w, \tag{23}$$

where $\mathbf{u}_{g,i} = \hat{\mathbf{z}} \times \nabla_H \psi_i$, $\omega_i = \nabla_H^2 \psi_i$, and where q_i and ψ_i are the QGPV and stream function for layer i respectively. $i = 1$ corresponds to the top layer, and $i = n$ corresponds to the bottom layer. ν is the Laplacian viscosity coefficient, r is the bottom friction coefficient, and Q_w is a term arising from an upper layer wind forcing.[4] δ_{ij} is the Kronecker delta. The multi-layer QGPV is given by:

$$q_1 = \nabla_H^2 \psi_1 + \beta y + s_1^+ (\psi_2 - \psi_1) \tag{24a}$$

$$q_i = \nabla_H^2 \psi_i + \beta y + s_i^- (\psi_{i-1} - \psi_i) + s_i^+ (\psi_{i+1} - \psi_i) \quad \text{for } 2 \le i \le n-1 \tag{24b}$$

$$q_n = \nabla_H^2 \psi_n + \beta y + s_n^- (\psi_{n-1} - \psi_n), \tag{24c}$$

where $n > 1$ has been assumed. The stratification parameters are given by:

$$s_i^\pm = \frac{f_0^2}{H_i g_{i\pm1/2}}, \tag{25}$$

where H_i is the thickness of layer i and where $g_{i+1/2}$ is the reduced gravity at the interface between layers i and $i+1$. Zero buoyancy boundary conditions have been applied on the upper and lower interfaces, corresponding to the potential vorticity δ-sheet boundary condition treatment described in Bretherton (1966).

The double gyre configuration described in Marshall et al. (2012) is used (see also Berloff et al. (2007) and Karabasov et al. (2009) for similar configurations). This is a three layer configuration in a square domain of size $L = 3840$ km, with wind forcing corresponding to:

$$Q_w = \begin{cases} -\dfrac{\tau_0}{\rho_0} \dfrac{2\pi}{H_1 L} A \sin\left(\pi \dfrac{\frac{L}{2} + y_\nu}{\frac{L}{2} + y_m}\right) & \text{if } y_\nu < y_m \\ \dfrac{\tau_0}{\rho_0} \dfrac{2\pi}{H_1 L} \dfrac{1}{A} \sin\left(\pi \dfrac{y_\nu - y_m}{\frac{L}{2} - y_m}\right) & \text{otherwise} \end{cases}. \tag{26}$$

where $x, y \in [0, L]$, $y_\nu = (y - L/2)$, and $y_m = B(x - L/2)$. $A = 0.9$ yields relatively increased wind forcing strength in the northern gyre, and $B = 0.2$ leads to a north-easterly tilt of the latitude of zero wind stress curl. A partial slip boundary condition (Haidvogel et al., 1992) is applied, $\nabla_H^2 \psi_i = -\nabla_H \psi \cdot \hat{\mathbf{n}}/\alpha$ on $\partial\Omega$, where $\hat{\mathbf{n}}$ is an outward unit normal on the boundary $\partial\Omega$ of the horizontal domain Ω, with a partial slip length scale of $1/\alpha = 120$ km. The stratification parameters are chosen so as to yield baroclinic deformation radii of 40 km and 23 km. Other parameters are as listed in Table 1. These parameters correspond to a Munk width of $\delta_M = (\nu/\beta)^{1/3} = 17.1$ km

[4] Q_w is related to the Ekman upwelling via $w_{Ek} = H_1 Q_w / f_0$.

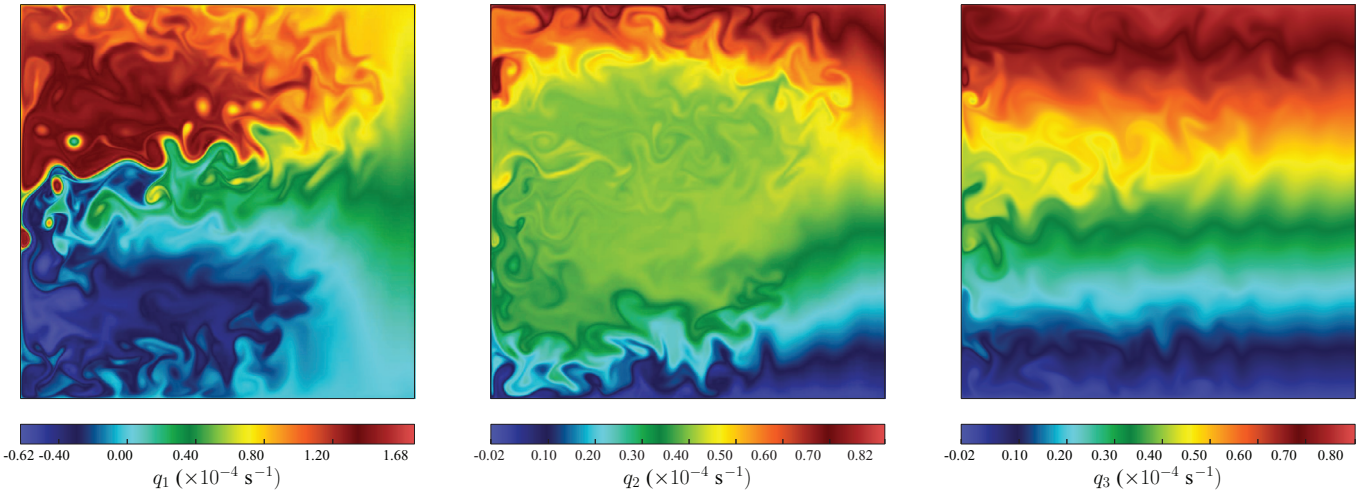

Fig. 1. The instantaneous potential vorticity for the upper layer (left), middle layer (centre), and lower layer (right) for the double gyre configuration after a 25,000 day integration from rest. Unless otherwise stated the colour bar limits in this and the following figures indicate the data range.

Table 1
Physical parameters for the double gyre configuration, as per Marshall et al. (2012).

Quantity	Symbol	Value(s)
Domain size	L	3840 km
Meridional planetary vorticity gradient	β	2×10^{-11} m^{-1} s^{-1}
Wind stress coefficient	τ_0	0.08 N m^{-2}
Viscosity coefficient	ν	100 m^2 s^{-1}
Bottom friction coefficient	r	4×10^{-8} s^{-1}
Partial slip length scale	$1/\alpha$	120 km
Layer thickness	H_1	0.25 km
	H_2	0.75 km
	H_3	3 km
Stratification parameters	$s_1^+ H_1 = s_2^- H_2$	2.965×10^{-7} m^{-1}
	$s_2^+ H_2 = s_3^- H_3$	5.603×10^{-7} m^{-1}
Reference density	ρ_0	1000 kg m^{-3}

and a Reynolds number relative to the Sverdrup velocity scale of $\mathrm{Re} = \tau_0/(\rho_0 \nu H_1 \beta) = 160$.

The equations are discretised in space using a finite element discretisation, with a conforming triangle mesh equipped with piecewise linear continuous basis functions for all fields ($P1$ discrete function spaces). A structured uniform grid with x- and y-direction vertex spacing of $\Delta x = 7.5$ km is used. The equations are discretised in time using third order Adams-Bashforth with a timestep size of $\Delta t = 20$ min. The model is implemented using the FEniCS system (Alnæs et al., 2009; 2014; Kirby, 2004; Kirby and Logg, 2006; Logg et al., 2012; Logg and Wells, 2010; Ølgaard and Wells, 2010) with the time discretisation handled using the approach described in Maddison and Farrell (2014). The model is described in further detail in Appendix B. In particular the model is constructed so that a discrete variant of the Taylor–Bretherton identity (Bretherton, 1966; Dritschel and McIntyre, 2008; Maddison and Marshall, 2013; Plumb, 1986; Taylor, 1915; Young, 2012) exists, thus ensuring the existence of a discrete flux-divergence relationship between eddy potential vorticity flux and eddy momentum stress.

The equations are integrated for a spinup period of 20,000 days, and diagnostics are computed over a further integration of 5,000 days. The mean is defined via a time mean over this latter 5,000 day window, and mean quantities are computed via the summation algorithm of Kahan (1965) (see also Higham (1993)). Fig. 1 shows the final potential vorticity, and Fig. 2 shows the mean stream function. The flow consists of a double-gyre, separated by a baroclinic jet which separates from the western boundary, and is populated by an active eddy field.

3.2. Force function budget

While this article is principally concerned with the force function associated with the eddy potential vorticity flux, it is possible nevertheless to define a force function for all terms in the QGPV equation, as described in Section 2.5. This is illustrated in Fig. 3, which shows the barotropic force functions associated with the upper layer wind forcing, the advection of planetary vorticity, and the advection of mean momentum. Sverdrup balance in the interior and inertial balance in the upstream jet are evident. The full force function budget was thus computed, and it was verified that the diagnosed budget was numerically closed.

3.3. Eddy force function

The eddy force function is shown in Fig. 4. The eddy force function due to the eddy Reynolds stress and eddy buoyancy flux are shown in Figs. 5 and 6 respectively[5]. The eddy Reynolds stress force function exhibits a dipole structure on either side of the downstream jet, with the sign indicating a positive forcing of the downstream mean jet in all layers. In the upstream region and in the upper and middle layers the dipole sign reverses, indicating a negative forcing of the upstream mean jet in these layers. The upper layer eddy buoyancy flux force function exhibits a quadrapole structure. Towards the northern boundary there is an anti-cyclonic forcing of the upper layer, balanced by a cyclonic forcing of the middle layer, while on the northern side of the downstream jet there is a cyclonic forcing of the upper layer, balanced by an anti-cyclonic forcing of the lower layer. This pattern is mirrored in the southern gyre. This structure indicates that the upper layer mean flow is decelerated by the eddy buoyancy fluxes towards the northern and southern boundaries (a downward flux of momentum input by the wind), but that the upper layer downstream mean jet is *accelerated* by the eddy buoyancy flux. The depth integrated buoyancy flux force function vanishes, reflecting the conservation of depth integrated momentum by the eddy buoyancy flux.

It follows directly from the definition (12) that a non-zero mean flow is accelerated by a force function if its gradient is oriented in the direction of the mean stream function gradient, and conversely that a

[5] There is an additional contribution to the eddy force function due to the eddy potential energy term arising from averaging of (B.2). This contribution is a small numerical artefact (which vanishes in the continuous case), with force function magnitude less than 0.0042 Sv yr^{-1} in all layers.

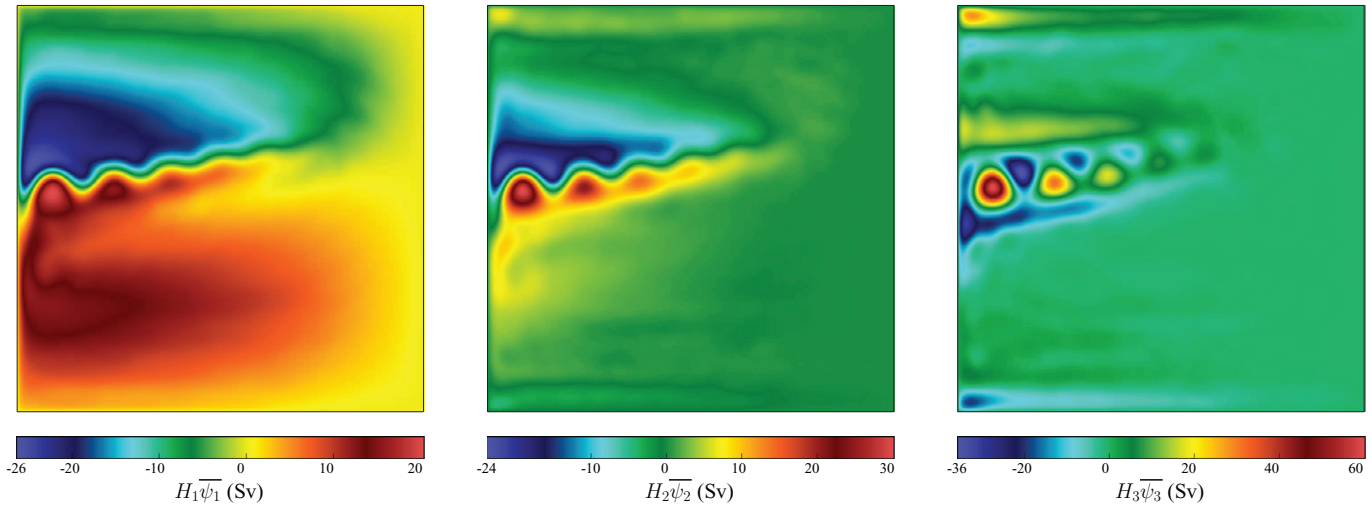

Fig. 2. The mean stream function for the upper layer (left), middle layer (centre), and lower layer (right), for the double gyre configuration, defined using a 5,000 day time mean after a 20,000 day spinup.

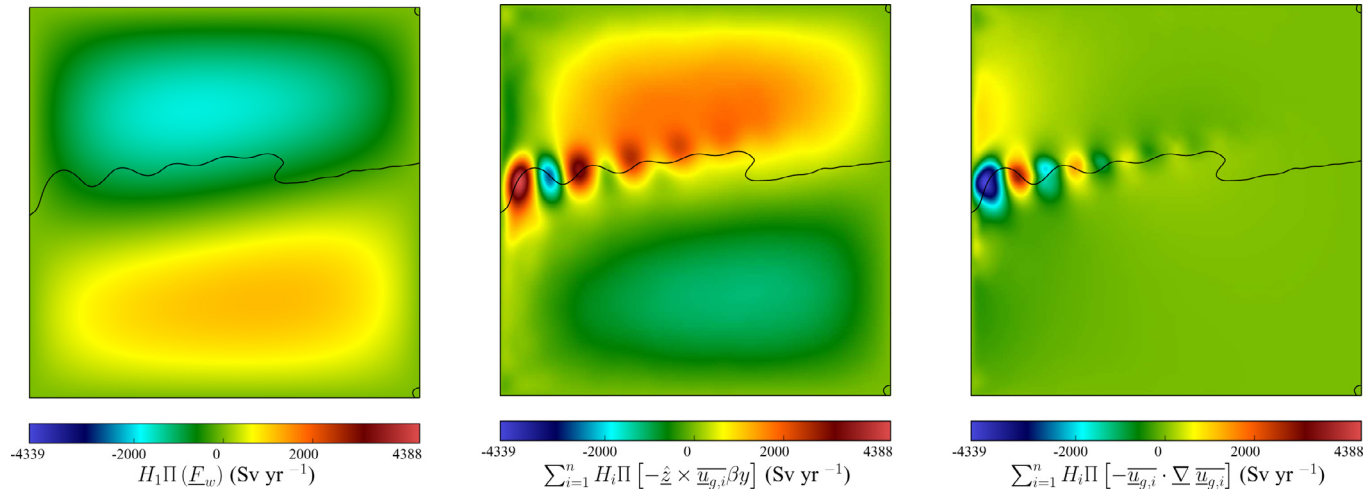

Fig. 3. The barotropic force function associated with the wind forcing (left), advection of planetary vorticity (centre), and advection of mean momentum (right), in units of Sverdrups per (Julian) year. A contour for the mean upper layer stream function is shown, with value equal to the upper layer stream function boundary value, to indicate the approximate location of the separating jet. These figures share a common colour scale.

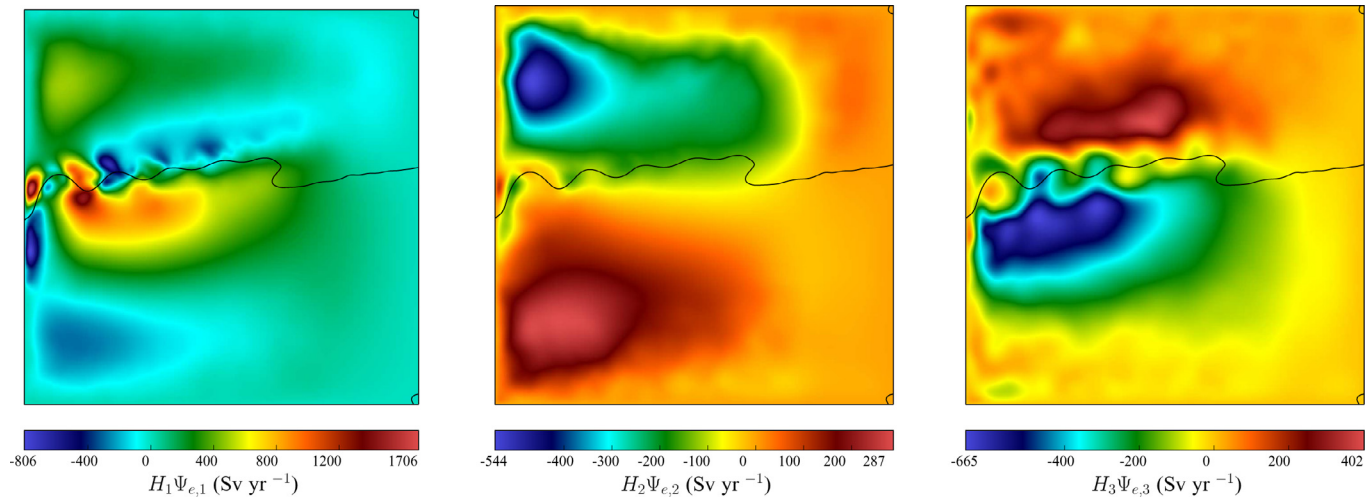

Fig. 4. The eddy force function in the upper layer (left), middle layer (centre), and lower layer (right). The mean stream function contour is as described in Fig. 3.

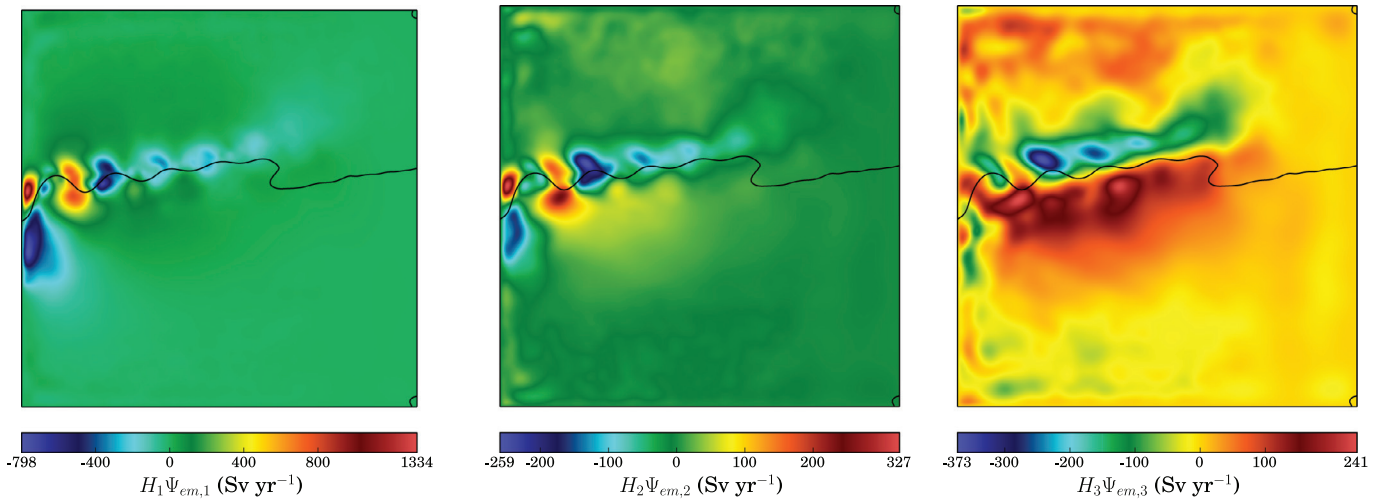

Fig. 5. The eddy force function due to eddy Reynolds stress in the upper layer (left), middle layer (centre), and lower layer (right). The mean stream function contour is as described in Fig. 3.

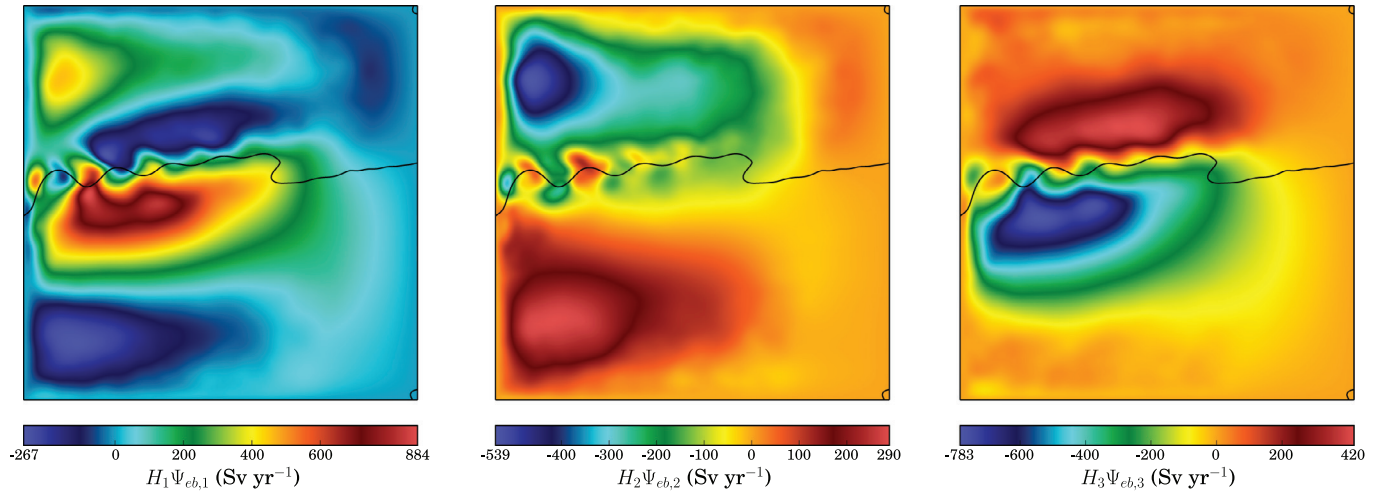

Fig. 6. The eddy force function due to eddy buoyancy flux in the upper layer (left), middle layer (centre), and lower layer (right). The mean stream function contour is as described in Fig. 3.

non-zero mean flow is decelerated by a force function if its gradient is oriented against the direction of the mean stream function gradient. This is reflected in the associated mean energy generation – given a potential vorticity flux $\mathbf{F}$ with an associated force function Ψ, the implied local mean energy generation per unit volume per unit time due to the divergent component of the flux is $\rho_0 \nabla_H \Psi \cdot \nabla_H \overline{\psi}$. The local mean energy generation due to the eddy Reynolds stress and eddy buoyancy flux force functions are shown in Figs. 7 and 8, and integrated energy generation is listed in Table 2.

In the domain integral the eddy Reynolds stress decreases the mean energy, with a total mean energy dissipation of 35 MW. This is consistent with global barotropic instability. However the eddy Reynolds stress force function indicates a significant generation of mean energy in the region of the downstream jet and, moreover, dissipation on the jet flanks. This suggests that the eddy Reynolds stress both accelerates and sharpens the jet, and is consistent with the action of up-gradient momentum fluxes in this region.

In the domain integral the eddy buoyancy flux also decreases the mean energy, with a total mean energy dissipation of 0.66 MW. The eddy buoyancy flux results in a dissipation of mean energy in the upper layer with a power of 5.7 MW, and a generation of mean energy in the middle and lower layers with powers of 2.9 MW and 2.1 MW respectively. This is consistent with the action of a downward flux of momentum, input by the wind, due to baroclinic instability. However the eddy buoyancy flux force function indicates a local generation of mean energy in the region of the downstream jet, particularly in the upper layer. This suggests that the downstream mean jet is forced both the eddy Reynolds stress (local barotropic stability) and through the eddy buoyancy flux (local baroclinic stability).

3.4. Zero normal divergent flux boundary conditions

An alternative horizontal Helmholtz decomposition for the eddy potential vorticity fluxes is considered:

$$\overline{\mathbf{u}_g' q'} = -\nabla_H \Psi_e^* + \hat{\mathbf{z}} \times \nabla_H \Phi_e^* + \hat{\mathbf{z}} \times \mathbf{H}_e^*, \tag{27}$$

where now zero normal flux boundary conditions are applied for the divergent component:

$$-\nabla_H \Psi_e^* \cdot \hat{\mathbf{n}} = 0, \tag{28}$$

where $\hat{\mathbf{n}}$ is an outward unit normal on the lateral boundaries of the domain.[6] The divergent eddy potential vorticity flux thus defined

[6] For the purposes of numerical calculations this boundary condition may lead to an ill posed problem. Instead the alternative boundary condition $(-\nabla_H \Psi_e^* - \overline{\mathbf{u}_g' q'}) \cdot \hat{\mathbf{n}} = 0$ is used. While the additional term vanishes identically for the continuous case, it is generally non-zero for a discrete model solution.

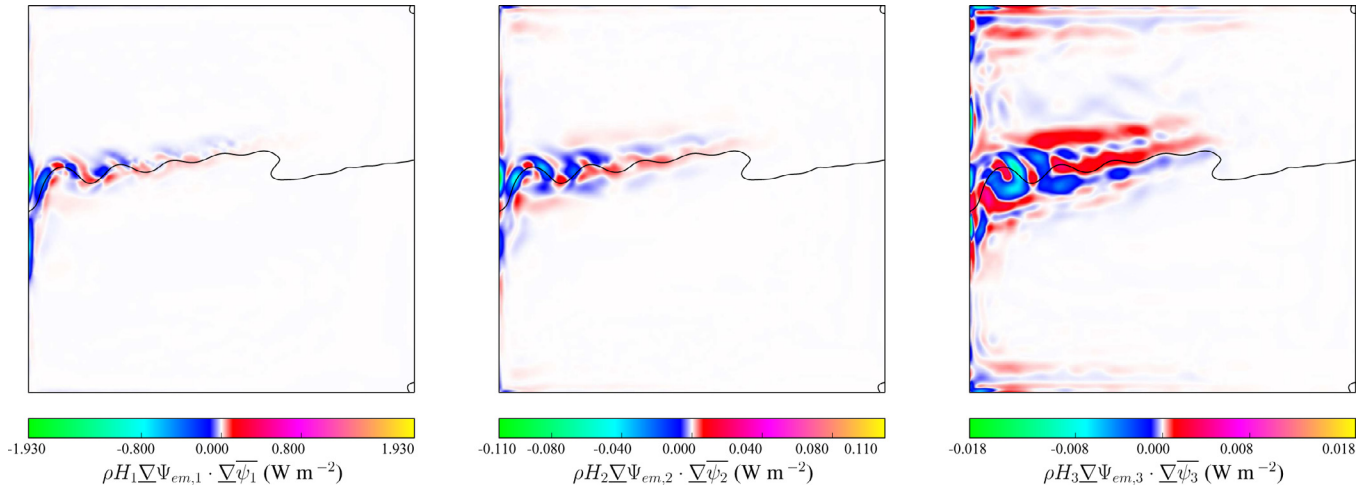

Fig. 7. The mean energy generation due to the divergent potential vorticity flux arising from the eddy Reynolds stress in the upper layer (left), middle layer (centre), and lower layer (right). The mean stream function contour is as described in Fig. 3. Symmetric colour scale bounds are used in these figures.

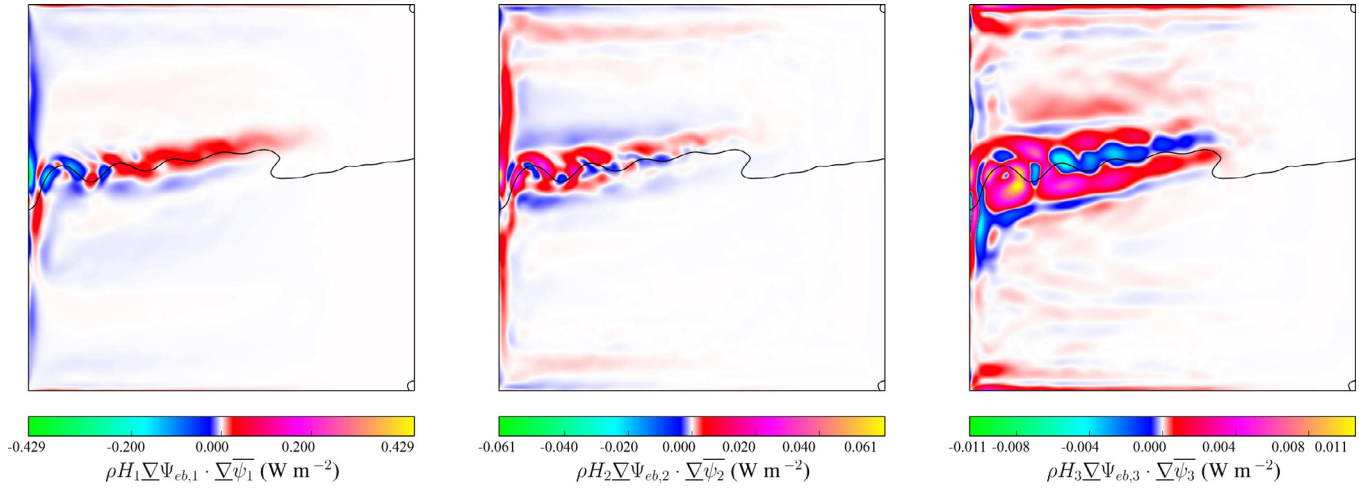

Fig. 8. The mean energy generation due to the divergent potential vorticity flux arising from the eddy buoyancy flux in the upper layer (left), middle layer (centre), and lower layer (right). The mean stream function contour is as described in Fig. 3. Symmetric colour scale bounds are used in these figures.

Table 2
Mean kinetic and potential energy, and the mean energy generation due to the divergent potential vorticity flux defined by the eddy Reynolds stress and eddy buoyancy flux force functions.

Layer	Mean kinetic energy (PJ)	Mean potential energy (PJ)	Eddy Reynolds stress forcing (MW)	Eddy buoyancy flux forcing (MW)
Upper	52	1,226	−31.9	−5.7
Middle	14	1,310	−2.3	+2.9
Lower	12	84	−0.4	+2.1
Total	77	2,619	−34.6	−0.7

therefore has the same (i.e. zero) normal component on the boundaries as the total eddy potential vorticity flux.[7] The resulting scalar potentials are shown in Fig. 9.

Let $\mathbf{D}_e = -\nabla_H \Psi_e$ refer to the divergent eddy potential vorticity flux defined by the eddy force function, and $\mathbf{D}_e^* = -\nabla_H \Psi_e^*$ refer to the divergent eddy potential vorticity flux which satisfies zero normal flux boundary conditions. As discussed in Section 2.4 the eddy force function yields the (horizontally oriented) divergent eddy potential vorticity flux which has a minimal L^2 norm. It can be seen from the values in Table 3 that $\mathbf{D}_e^*$ has a significantly larger L^2 norm than $\mathbf{D}_e$ in all layers and hence is, by this definition, significantly sub-optimal. That is, $\mathbf{D}_e^*$ includes a harmonic component which is successfully removed in the definition of $\mathbf{D}_e$.

The consequences of the additional harmonic component can be seen in Fig. 10, which shows the two divergent potential vorticity fluxes in the middle layer. $\mathbf{D}_{e,2}$ indicates a clear eddy potential vorticity flux convergence in the northern gyre and eddy potential vorticity flux divergence in the southern gyre. This pattern is evident in $\mathbf{D}_{e,2}^*$, but is obscured, particularly on the eastern side of the domain.

3.5. Potential vorticity mixing

A mesoscale eddy parameterisation typically specifies (or at least implies) a parameterised approximation for the eddy potential vorticity flux $\overline{\mathbf{u}_g' q'}$. However, as only the divergence of this flux appears in the prognostic QGPV Eq. (10), a direct comparison of parameterised and diagnosed eddy potential vorticity fluxes cannot be used to measure the performance of a parameterisation. While the parameterised eddy potential vorticity flux may differ from that measured diagnostically, the parameterisation may still perform well if the potential vorticity flux *divergence* is well approximated. Equivalently, it is possible to re-interpret any given parameterised eddy potential vorticity flux as a parameterisation not for the full eddy potential vorticity flux, but an appropriate divergent component.

[7] This boundary condition defines Ψ_e^* up to an arbitrary function of z and t (which does not affect the implied divergent flux), and this additional freedom is removed by imposing $\Psi_e^* = 0$ at $x = 0$ and $y = 0$.

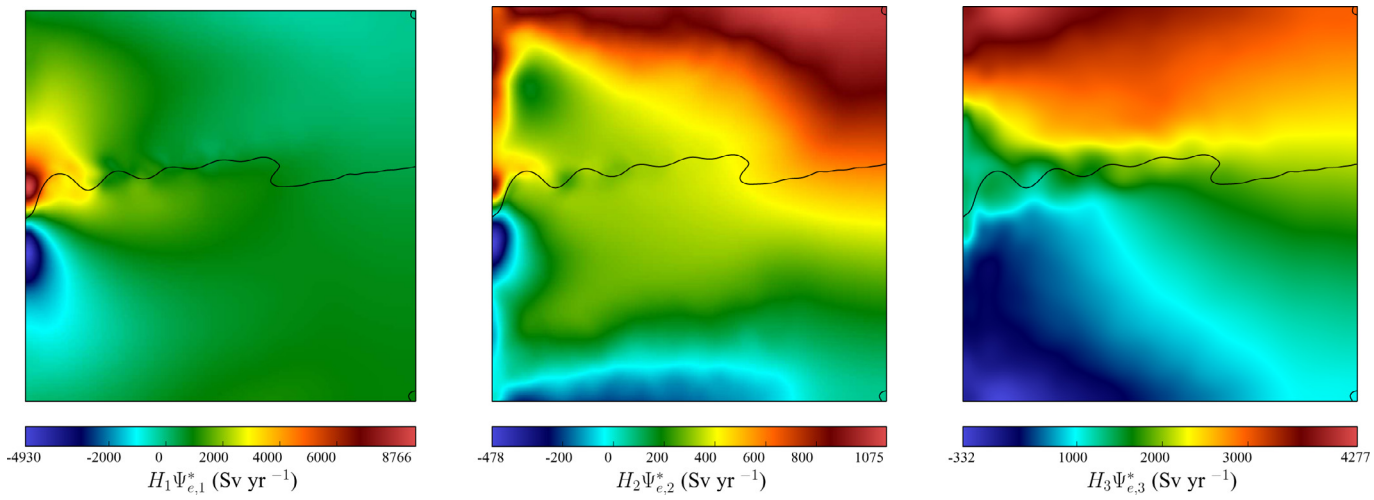

Fig. 9. The scalar potential Ψ^*_e for the divergent eddy potential vorticity flux, defined using zero normal flux boundary conditions, in the upper layer (left), middle layer (centre), and lower layer (right). The mean stream function contour is as described in Fig. 3.

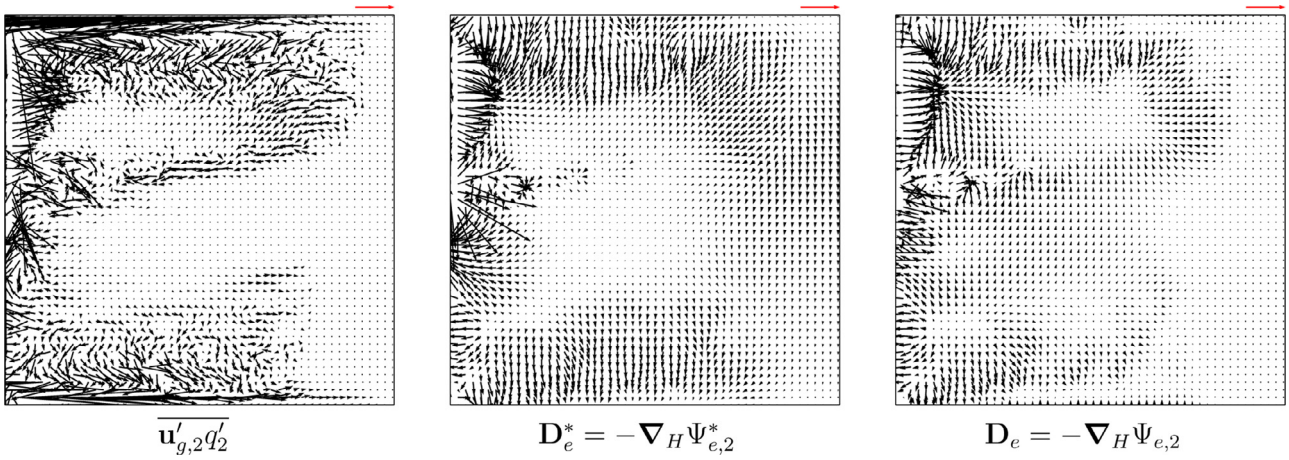

Fig. 10. Middle layer potential vorticity flux vectors. Left: full eddy potential vorticity flux. Centre: divergent eddy potential vorticity flux defined using a horizontal Helmholtz decomposition with zero normal divergent flux boundary conditions. Right: divergent eddy potential vorticity flux defined using the eddy force function. Every tenth value (in each direction) of the vector fields are shown, with the red vector indicating a magnitude of 10^{-5} cm s^{-2}. (For interpretation of the references to colour in this figure legend, the reader is referred to the web version of this article.)

Table 3
Normalised L^2 norm of the eddy potential vorticity flux in each layer, and of divergent components of the eddy potential vorticity flux defined using zero normal flux boundary conditions $-\nabla_H\Psi^*_e$, and using the eddy force function $-\nabla_H\Psi_e$. The percentages in brackets indicate the ratio of a divergent potential vorticity flux norm to the total potential vorticity flux norm in a given layer. The normalised L^2 norm is, for a vector field $\mathbf{v}$, given by $\|\mathbf{v}\| = \sqrt{\int_\Omega \mathbf{v}\cdot\mathbf{v}}/\sqrt{\int_\Omega 1}$, where Ω is the horizontal domain.

Layer	$\left\|\overline{\mathbf{u}'_{g,i}q'_i}\right\|$ (cm s^{-2})	$\left\|\mathbf{D}^*_{e,i}\right\| = \left\|\nabla_H\Psi^*_{e,i}\right\|$ (cm s^{-2})	$\|\mathbf{D}_{e,i}\| = \|\nabla_H\Psi_{e,i}\|$ (cm s^{-2})
Upper	2.86×10^{-4}	4.21×10^{-5} (14.7%)	2.24×10^{-5} (7.8%)
Middle	8.75×10^{-6}	2.46×10^{-6} (28.1%)	1.82×10^{-6} (20.8%)
Lower	3.02×10^{-6}	1.22×10^{-6} (40.6%)	7.08×10^{-7} (23.5%)

This issue can be resolved by comparing parameterised and diagnosed eddy potential vorticity flux divergences directly. However the eddy potential vorticity flux divergence is typically a noisy field, resulting from the differentiation required for its calculation. The eddy force function depends only upon the eddy potential vorticity flux divergence, but the inverse elliptic operator inherent in its definition ensures that this is a much smoother field. Moreover the optimality property discussed in Section 2.4 and Appendix A ensures that, among all possible scalar potentials (defined using alternative boundary conditions), there is a well defined sense in which the eddy force function is the smoothest – it yields the scalar potential with minimum gradient (specifically the eddy force function is a scalar potential with minimum H^1_0 semi-norm). Hence the eddy force function provides a natural means of comparing parameterised and diagnosed eddy potential vorticity fluxes.

A down-gradient potential vorticity mixing parameterisation is considered:

$$\overline{\mathbf{u}'_g q'} = -\kappa\nabla_H\bar{q}, \tag{29}$$

where κ is the eddy potential vorticity diffusivity[8]. The utility of the force function is illustrated for a basic potential vorticity mixing parameterisation, with a layer-wise constant eddy diffusivity

[8] Note that even with a constant diffusivity this does not imply that the divergent part of the flux, defined using the force function, is equal to $-\kappa\nabla_H\bar{q}$, as $\bar{q}$ is not equal to a constant on the boundary.

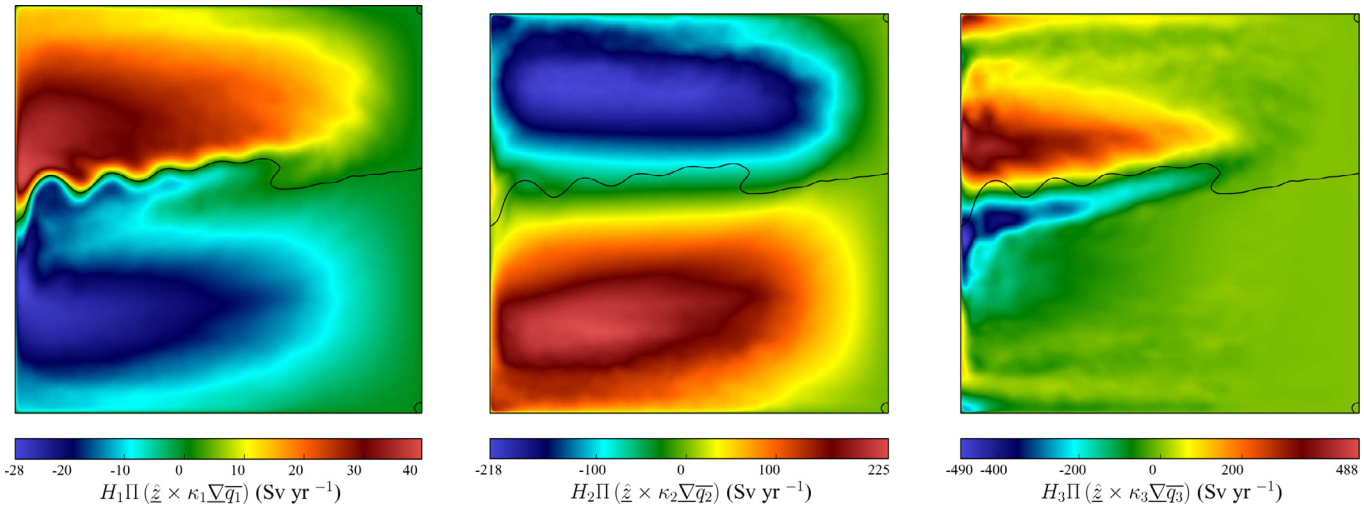

Fig. 11. Parameterised eddy force functions resulting from a down-gradient potential vorticity mixing parameterisation with a constant eddy potential vorticity diffusivity in each layer. The diffusivities are chosen so as to minimise the L^2 mismatch between the parameterised and diagnosed eddy force functions in each layer. The mean stream function contour is as described in Fig. 3.

Table 4
L^2 optimal constant eddy potential vorticity diffusivies, which minimise the L^2 mismatch between parameterised and diagnosed eddy force functions in each layer. The normalised L^2 norm is, for a vector field $\mathbf{v}$, given by $\|\mathbf{v}\| = \sqrt{\int_\Omega \mathbf{v}\cdot\mathbf{v}}/\sqrt{\int_\Omega 1}$, where Ω is the horizontal domain.

Layer	Eddy diffusivity κ_i ($m^2\ s^{-1}$)	Normalised L^2 error $\left\|\Pi\left(\hat{\mathbf{z}}\times\kappa_i\nabla_H\bar{q}_i\right)-\Psi_{e,i}\right\|$ (Sv yr^{-1})	Relative L^2 error $\left\|\Pi\left(\hat{\mathbf{z}}\times\kappa_i\nabla_H\bar{q}_i\right)-\Psi_{e,i}\right\|/\|\Psi_{e,i}\|$
Upper	46	263	99.8%
Middle	481	78	54.2%
Lower	−789	160	84.5%

considered. The parameterisation is not expected to perform well without allowing for some spatial variation of the diffusivity, but this enables the straightforward derivation of optimal constant diffusivities in each layer which minimise the L^2 mismatch between the parameterised and diagnosed eddy force functions.

The resulting parameterised eddy force functions are shown in Fig. 11, and the diffusivities are listed in Table 4. The middle layer parameterised eddy force function is able to represent the diagnosed eddy force function with a relative L^2 error of 54.2%. This is rather encouraging – even a basic constant eddy diffusivity is able to achieve a partial representation of the eddy force function. However the upper layer parameterised eddy force function matches the diagnosed eddy force function poorly, with a relative L^2 error of 99.8%. That is, in the upper layer the parameterised eddy force function is very nearly L^2 orthogonal to the diagnosed eddy force function, and the mean potential vorticity gradient is providing little information on the structure of the eddy force function here. The lower layer L^2 mismatch has an intermediate value of 84.5%, although the diffusivity is negative.

4. Conclusions

The consideration of the dynamical influence of eddy fluxes in the ocean and atmosphere is always complicated by the need to consider the possible presence of rotational fluxes, which in practice can be large and obscure any underlying divergent component. A meaningful decomposition into divergent and rotational components, while intuitively desirable, is in general difficult to achieve – it must necessarily involve a choice among a family of valid decompositions, which differ through a choice of boundary conditions.

In this article this issue has been addressed by relating non-divergent momentum tendencies to eddy potential vorticity fluxes. The momentum equation comes ready equipped with a Helmholtz decomposition, including a unique choice of boundary condition, either through the definition of the non-divergent velocity or through the definition of the pressure. Since potential vorticity fluxes are derived from the momentum and thermodynamic equations, the Helmholtz decomposition provided by the momentum equation, including the associated boundary condition, can be carried through to the potential vorticity equation, yielding a decomposition of potential vorticity fluxes.

This procedure has been applied to the quasi-geostrophic equations. The definition of the quasi-geostrophic stream function provides a boundary condition for the horizontal Helmholtz decomposition of the total momentum tendency in the quasi-geostrophic residual-mean equation. This can be used to define a stream function tendency, or "force function", which in turn defines the non-divergent component of the total momentum tendency. The tendency can be directly related to a potential vorticity flux, and the force function then defines the divergent component of this flux. A unique decomposition for individual potential vorticity fluxes is arrived at by asserting that the decomposition should be linear – in particular this asserts that one should be able to resolve force functions (or equivalently non-divergent momentum tendencies) via direct summing. The divergent component of the eddy potential vorticity flux thus defined satisfies a zero tangential component boundary condition.

This results in a unique Helmholtz decomposition for eddy potential vorticity fluxes, with an explicit relation between the divergent eddy potential vorticity flux and the eddy momentum forcing. There is therefore an immediate intuitive link between the dynamically active divergent component of the eddy potential vorticity flux and the local forcing of the mean flow. In a simply connected domain this approach results in the unique (horizontally oriented) divergent eddy potential vorticity flux with minimum L^2 norm, and hence there is a well-defined sense in which the decomposition is optimal, and

extracts the smallest possible underlying divergent eddy potential vorticity flux.

The decomposition has been applied to eddy potential vorticity fluxes diagnosed from a three-layer quasi-geostrophic model. Expected features of the eddy-mean-flow interaction were identified. The eddy Reynolds stress force function indicated a forcing of the mean jet, consistent with the action of up-gradient momentum fluxes. In some parts of the domain the eddy buoyancy flux force function indicated a downward flux of momentum input by the wind, although local forcing of the upper layer downstream mean jet was observed. These diagnostics suggested that the mean jet was forced through both local barotropic and baroclinic stability, although the system was found to be globally both barotropically and baroclinically unstable.

The decomposition has been compared against an alternative Helmholtz decomposition of potential vorticity fluxes, with zero normal divergent flux boundary conditions. This latter decomposition lacks a direct relationship between divergent potential vorticity fluxes and local mean momentum forcing, obscuring the interpretation. In a simply connected domain it also necessarily defines a larger divergent component (in an L^2 sense) than that defined using the eddy force function, obscuring structure in the resulting divergent potential vorticity fluxes.

Finally it has been proposed that the eddy force function is suitable for assessment and comparison of eddy parameterisations. The need to consider rotational flux components means that it is not appropriate to compare parameterised and diagnosed eddy potential vorticity fluxes directly, but rather some comparison based upon potential vorticity flux divergences must be considered. The potential vorticity flux divergence itself is a noisy field, due to the differentiation inherent in its definition. However the eddy force function, which is directly related to the eddy potential vorticity flux divergence through a linear operator, is a much smoother field. Indeed in a simply connected domain it is, among all possible scalar potentials defining a divergent eddy potential vorticity flux, a potential with minimum H_0^1 semi-norm, and hence in this sense is the smoothest.

Parameterised and diagnosed eddy force functions were compared for a basic down-gradient potential vorticity flux closure with a constant eddy diffusivity. The results were very encouraging in the middle layer, where even the use of a constant diffusivity yielded partial agreement. However in the upper layer the parameterised and diagnosed eddy force functions were very nearly orthogonal (in an L^2 sense), suggesting that, in a down-gradient potential vorticity flux parameterisation in this layer, much of the structure of the eddy fluxes must be represented not by the mean potential vorticity gradient, but by the eddy diffusivity. A detailed analysis which considers spatially varying diffusivities is the subject of an in-preparation article.

While it is suggested that H_0^1 optimality of the eddy force function is useful from the perspective of parameterisation assessment, it should be noted that the corresponding local divergent eddy fluxes cannot be used directly to infer a local potential vorticity diffusivity. Specifically, the eddy enstrophy equation is (assuming Φ_e can be defined so that the harmonic component $\mathbf{H}_e = \mathbf{0}$):

$$\begin{aligned}\partial_t \overline{\Lambda} + \nabla \cdot (\overline{\mathbf{u}_g \Lambda}) &= -\overline{\mathbf{u}_g' q'} \cdot \nabla_H \overline{q} + R \\ &= \nabla_H \Psi_e \cdot \nabla_H \overline{q} - (\hat{\mathbf{z}} \times \nabla \Phi_e) \cdot \nabla_H \overline{q} + R, \end{aligned} \tag{30}$$

where $\Lambda = q'q'/2$ and where R includes forcing and dissipation. Integration and application of no-normal-flow boundary conditions leads to:

$$\partial_t \int_\Omega \overline{\Lambda} = \int_\Omega \nabla_H \Psi_e \cdot \nabla_H \overline{q} - \int_{\partial\Omega} \overline{q} (\hat{\mathbf{z}} \times \nabla \Phi_e) \cdot \hat{\mathbf{n}} + \int_\Omega R. \tag{31}$$

The second right-hand-side term need not vanish, and hence in a statistically steady state there is no requirement for the first and third terms on the right-hand-side to balance. An alternative, and appropriately invariant, form is:

$$\partial_t \int_\Omega \overline{\Lambda} = \int_\Omega \overline{q} \nabla_H^2 \Psi_e + \int_\Omega - R, \tag{32}$$

although this does not suggest a local method for diagnosing a diffusivity. Note that for the decomposition subject to zero normal divergent flux boundary conditions the corresponding boundary integral does vanish:

$$\partial_t \int_\Omega \overline{\Lambda} = \int_\Omega \nabla_H \Psi_e^* \cdot \nabla_H \overline{q} + \int_\Omega R. \tag{33}$$

The approach described in this article can be generalised to the hydrostatic primitive equations via application of the decomposition of Marshall and Pillar (2011). In this case vector force functions are defined and, carrying the corresponding non-divergent momentum tendencies through to the Ertel potential vorticity equation, this defines filtered Ertel potential vorticity fluxes. While in the general this does not define a Helmholtz decomposition of the potential vorticity fluxes (the resulting filtered potential vorticity fluxes are not generally curl free) this nevertheless yields dynamically consistent filtered potential vorticity fluxes with a simple intuitive relation to local momentum forcing.

Note that, as pointed about by Fox-Kemper (pers. comms.), we have here considered only the dynamically active divergent component of fluxes of potential vorticity. For the very special case of the quasi-geostrophic equations subject to zero buoyancy boundary conditions on the upper and lower surfaces, an intuitive divergent component of the eddy buoyancy fluxes can be defined (see Appendix C). For more general cases, as discussed in Bachman and Fox-Kemper (2013), the non-uniqueness of divergent eddy fluxes remains, and the approach described in this article does not appear to provide much guidance.

Since eddy enstrophy is dissipated on small scales it is known that the eddy potential vorticity flux and mean potential vorticity gradient must on average be anti-correlated (that is, their L^2 inner product is negative). In this sense eddy fluxes must be down-gradient on average, and hence must mix potential vorticity on average. Considerable effort has previously been invested in studying the degree to which the eddy potential vorticity flux is locally oriented down-gradient, but the inherent freedom to remove arbitrary dynamically inactive rotational fluxes means that this analysis is fraught with ambiguity. This issue affects the study of eddy parameterisations more generally – if only divergent fluxes are to be parameterised, then it must first be decided *which* divergent flux is relevant. Here it is proposed that the divergent flux be defined in a manner consistent with the link between the momentum and potential vorticity dynamics. This yields a smooth eddy force function which it is further proposed is suitable for assessment of parameterised eddy potential vorticity flux divergences.

Acknowledgements

JRM acknowledges helpful discussion with Colin J. Cotter regarding the treatment of the partial-slip boundary condition with an explicit time discretisation described in Appendix B, Pavel S. Berloff for assistance with a finite difference quasi-geostrophic code on which the finite element code discussed in this paper is based, and Julian Mak for comments on the manuscript. This work was funded by the U.K. Natural Environment Research Council (NE/H020454/1, NE/I015345/1, and NE/L005166/1) and Engineering and Physical Sciences Research Council (EP/G036136/1). Data from the example in Section 3 is available through Edinburgh DataShare (doi:10.7488/ds/203). The authors thank B. Fox-Kemper and an anonymous reviewer for comments which significantly improved this article.

Appendix A. The L^2 minimal divergent eddy potential vorticity flux

Consider a horizontal Helmholtz decomposition of the eddy potential vorticity flux

$$\overline{\mathbf{u}_g' q'} = -\nabla_H \Psi_e^* + \hat{\mathbf{z}} \times \nabla_H \Phi_e^* + \hat{\mathbf{z}} \times \mathbf{H}_e^*, \tag{A.1}$$

The divergent potential vorticity flux, $-\nabla_H \Psi_e^*$, is defined by the scalar potential Ψ_e^*, which is a solution of the Poisson equation

$$\nabla_H^2 \Psi_e^* = -\nabla_H \cdot \overline{\mathbf{u}_g' q'}. \tag{A.2}$$

Consider weak solutions $\Psi_e^* \in H^1(\Omega)$ which satisfy

$$\int_\Omega \nabla_H \zeta \cdot \nabla_H \Psi_e^* = -\int_\Omega \nabla_H \zeta \cdot \overline{\mathbf{u}_g' q'} \quad \forall \zeta \in H_0^1(\Omega), \tag{A.3}$$

where Ω is the horizontal domain. In this appendix it is proved that, among all such weak solutions, homogeneous Dirichlet boundary conditions in the problem for Ψ_e^* yield the unique divergent potential vorticity flux $-\nabla_H \Psi_e^*$ which has minimal L^2 norm. That is, up the addition of an arbitrary function of z and t (which has zero horizontal gradient), there exists a unique solution to (A.3) which minimises $\sqrt{\int_\Omega \nabla_H \Psi_e^* \cdot \nabla_H \Psi_e^*}$, and moreover this optimal solution is equal to a constant on all boundaries. This optimality property follows from the following:

Lemma. *Let $\Omega \subset \mathbb{R}^d$, $\mathbf{F} \in [L^2(\Omega)]^d$, and consider a real Hilbert space $U \subseteq H^1(\Omega)$. Define the following:*

$$V = \left\{ \phi \in U : \int_\Omega \phi = 0 \right\} \tag{A.4a}$$

$$V_0 = U \cap H_0^1(\Omega) \tag{A.4b}$$

$$V_1 = \left\{ \phi \in U : \int_\Omega \nabla \zeta \cdot \nabla \phi = 0 \quad \forall \zeta \in V_0 \right\} \tag{A.4c}$$

$$W = \left\{ \phi \in V : \int_\Omega \nabla \zeta \cdot \nabla \phi = \int_\Omega \nabla \zeta \cdot \mathbf{F} \quad \forall \zeta \in V_0 \right\}. \tag{A.4d}$$

Then there exists a unique $\phi \in W$ *which minimises the functional* $J : W \to \mathbb{R}$ *where:*

$$J(\phi) = \|\phi\|_{H_0^1}^2 = \|\nabla \phi\|_{L^2}^2 = \int_\Omega \nabla \phi \cdot \nabla \phi. \tag{A.5}$$

Moreover there exists a unique $c \in \mathbb{R}$ such that $\phi + c \in V_0$.

Proof. All $\phi \in W$ can be separated into particular and homogeneous parts, $\phi = \phi_0 + \phi_1$, where $\phi_0 \in V_0$ and $\phi_1 \in V_1$. Then

$$\begin{aligned}
&\int_\Omega \nabla \zeta \cdot \nabla \phi = \int_\Omega \nabla \zeta \cdot \mathbf{F} \quad \forall \zeta \in V_0 \\
\iff \quad &\int_\Omega \nabla \zeta \cdot \nabla \phi_0 + \int_\Omega \nabla \zeta \cdot \nabla \phi_1 = \int_\Omega \nabla \zeta \cdot \mathbf{F} \quad \forall \zeta \in V_0 \\
\iff \quad &\int_\Omega \nabla \zeta \cdot \nabla \phi_0 = \int_\Omega \nabla \zeta \cdot \mathbf{F} \quad \forall \zeta \in V_0,
\end{aligned}$$

where the final line follows from the definition of V_1. By the Lax-Milgram lemma this is satisfied by a unique $\phi_0 \in V_0$. Now define a functional $\hat{J} : V_1 \to \mathbb{R}$ where

$$\hat{J}(\phi_1') = \int_\Omega \nabla(\phi_0 + \phi_1') \cdot \nabla(\phi_0 + \phi_1'). \tag{A.6}$$

This functional is minimised if and only if the Gâteaux derivative vanishes in all directions $\eta \in V_1$

$$\begin{aligned}
&d\hat{J}(\phi_1'; \eta) = 0 \quad \forall \eta \in V_1 \\
\iff \quad &\int_\Omega \nabla \eta \cdot \nabla \phi_0 + \int_\Omega \nabla \eta \cdot \nabla \phi_1' = 0 \quad \forall \eta \in V_1 \\
\iff \quad &\int_\Omega \nabla \eta \cdot \nabla \phi_1' = 0 \quad \forall \eta \in V_1 \\
\iff \quad &\int_\Omega \nabla \phi_1' \cdot \nabla \phi_1' = 0.
\end{aligned}$$

where the penultimate line follows from the definition of V_1. Hence the ϕ_1' which minimise $\hat{J}$ are L^2 equivalent to constant functions. $\phi = \phi_0 + \phi_1 \in W$ implies that J is minimised by $\phi_1 = -\int_\Omega \phi_0$. Hence a unique $\phi \in W$ minimises J, and moreover $\phi + \int_\Omega \phi_0 \in V_0$. □

Appendix B. Multi-layer quasi-geostrophic model

The Taylor–Bretherton identity relates eddy potential vorticity flux to eddy momentum stress (Bretherton, 1966; Dritschel and McIntyre, 2008; Maddison and Marshall, 2013; Plumb, 1986; Taylor, 1915; Young, 2012). Unaveraged (relative) potential vorticity flux and momentum stress can be similarly related, allowing the multi-layer QGPV equation to be written in the following form:

$$\partial_t q_i + \nabla_H \cdot \left(\mathbf{f}_i + \mathbf{u}_{g,i} \beta y \right) = \nu \nabla_H^2 \omega_i - r \delta_{in} \omega_i + \delta_{i1} Q_w, \tag{B.1}$$

where symbols are as defined in Section 3.1 and where the potential vorticity flux $\mathbf{f}_i$ has x- and y-components

$$f_{x,i} = \partial_x N_i + \partial_y (M_i + P_i) + \frac{R_{i-1/2} - R_{i+1/2}}{H_i} \tag{B.2a}$$

$$f_{y,i} = \partial_x (M_i - P_i) - \partial_y N_i + \frac{S_{i-1/2} - S_{i+1/2}}{H_i}, \tag{B.2b}$$

with advective momentum flux components

$$M_i = \frac{1}{2}\left(v_{g,i}^2 - u_{g,i}^2 \right) \tag{B.3a}$$

$$N_i = u_{g,i} v_{g,i}, \tag{B.3b}$$

potential energy

$$P_1 = \frac{1}{4} s_1^+ (\psi_2 - \psi_1)^2 \tag{B.4a}$$

$$P_i = \frac{1}{4}\left[s_i^- (\psi_{i-1} - \psi_i)^2 + s_i^+ (\psi_{i+1} - \psi_i)^2 \right] \quad \text{for } 2 \le i \le n-1 \tag{B.4b}$$

$$P_n = \frac{1}{4} s_n^- (\psi_{n-1} - \psi_n)^2, \tag{B.4c}$$

and advective buoyancy flux components:

$$R_{1/2} = R_{n+1/2} = S_{1/2} = S_{n+1/2} = 0 \tag{B.5a}$$

$$R_{i+1/2} = \frac{1}{2}\left(u_{g,i} + u_{g,i+1} \right) H_i s_i^+ (\psi_i - \psi_{i+1}) \quad \text{for } 1 \le i \le n-1 \tag{B.5b}$$

$$S_{i+1/2} = \frac{1}{2}\left(v_{g,i} + v_{g,i+1} \right) H_i s_i^+ (\psi_i - \psi_{i+1}) \quad \text{for } 1 \le i \le n-1. \tag{B.5c}$$

$u_{g,i}$ and $v_{g,i}$ are the x- and y- components of $\mathbf{u}_{g,i}$, respectively. The potential vorticity flux $\mathbf{f}_i$ thus defined is a (vertically discrete) divergence of a (vertically discrete) rank two momentum stress tensor. Averaging of these equations leads to a vertically discrete Taylor–Bretherton identity.

Given discrete function spaces $V \subset H^1(\Omega)$ and $V_0 = V \cap H_0^1(\Omega)$, and considering times $t \in [0, \tau]$, the equations are discretised in space via the following semi-discrete formulation:

Find $q_i \in V \times C^1([0, \tau])$ such that

$$\begin{aligned}
&\int_\Omega \phi_0 \partial_t q_i - \int_\Omega \nabla_H \phi_0 \cdot \left(\mathbf{f}_i + \mathbf{u}_{g,i} \beta y \right) \\
&\quad = -\int_\Omega \nabla_H \phi_0 \cdot \nu \nabla_H \omega_i - \int_\Omega \phi_0 \delta_{in} r \omega_i \\
&\qquad + \int_\Omega \phi_0 \delta_{i1} Q_w \quad \forall \phi_0 \in V_0, i \in \{1, \dots, n\}
\end{aligned} \tag{B.6a}$$

Find $\psi_i \in \{ v \in V \times C^0([0, \tau]) : v - c_i \in V_0$
$\times C^0([0, \tau])\}, c_i \in C^0([0, \tau])$ such that:

$$-\int_\Omega \nabla_H\phi_0\cdot\nabla_H\psi_1+\int_\Omega \phi_0 s_1^+(\psi_2-\psi_1)$$
$$=\int_\Omega \phi_0(q_1-\beta y)\quad \forall\phi_0\in V_0 \tag{B.6b}$$

$$-\int_\Omega \nabla_H\phi_0\cdot\nabla_H\psi_i+\int_\Omega \phi_0[s_i^-(\psi_{i-1}-\psi_i)+s_i^+(\psi_{i+1}-\psi_i)]$$
$$=\int_\Omega \phi_0(q_i-\beta y)\quad \forall\phi_0\in V_0, i\in\{2,\dots,n-1\} \tag{B.6c}$$

$$-\int_\Omega \nabla_H\phi_0\cdot\nabla_H\psi_n+\int_\Omega \phi_0 s_n^-(\psi_{n-1}-\psi_n)$$
$$=\int_\Omega \phi_0(q_n-\beta y)\quad \forall\phi_0\in V_0 \tag{B.6d}$$

$$\sum_{i=1}^n H_i\psi_i\in V_0\times C^0([0,\tau]) \tag{B.6e}$$

$$\int_\Omega \frac{2(\psi_{i+1}-\psi_i)}{H_i+H_{i+1}}=0\quad \forall i\in\{1,\dots,n-1\} \tag{B.6f}$$

Find $\omega_i\in V\times C^0([0,\tau])$ such that

$$\int_\Omega \phi\omega_i+\int_{\partial\Omega}\phi\frac{1}{\alpha}\omega_i=-\int_\Omega \nabla_H\phi\cdot\nabla_H\psi_i\quad \forall\phi\in V, i\in\{1,\dots,n\} \tag{B.6g}$$

where $\partial\Omega$ is the boundary of the horizontal domain Ω. A discrete potential vorticity flux and discrete momentum stress are defined via continuous Galerkin discretisations of (B.2)–(B.5).

The partial slip boundary condition (Haidvogel et al., 1992) is applied weakly on ω_i in (B.6g). The partial slip boundary condition is implicitly imposed weakly on q_i via (B.6a), (24), and (B.6g) (see Barrett (1978); Campion-Renson and Crochet (1978), Gresho and Sani (2000, section 3.12.4) for related discussions on boundary conditions for the weak form 2D stream function-vorticity equations). The no-normal-flow boundary condition is applied strongly in (B.6b)–(B.6d), and a homogeneous Dirichlet boundary condition is applied strongly on the barotropic stream function via (B.6e). Mass conservation (McWilliams, 1977); (Pedlosky, 1987, section 3.25) is imposed via (B.6f).

The equations are discretised in time using third order Adams-Bashforth, started with a forward Euler step and a second order Adams-Bashforth step, yielding second order accuracy in time. The partial slip boundary condition is treated by first computing $q_i^{*,m}\in V$, which do not satisfy the partial slip boundary condition, via:

Find $G_i^{*,m}\in V$ such that:

$$\int_\Omega \phi G_i^{*,m}-\int_\Omega \nabla_H\phi\cdot\left(\mathbf{f}_i^m+\mathbf{u}_{g,i}^m\beta y\right)=-\int_\Omega \nabla_H\phi\cdot\nu\nabla_H\omega_i^m$$
$$-\int_\Omega \phi\delta_{in}r\omega_i^m+\int_\Omega \phi\delta_{i1}Q_w\quad \forall\phi\in V, i\in\{1,\dots,n\} \tag{B.7a}$$

$$q_i^{*,m+1}=q_i^m+\Delta t\sum_{j=0}^{M-1}\gamma_j G_i^{*,m-j}\quad \forall i\in\{1,\dots,n\}, \tag{B.7b}$$

where a superscript m indicates a field at discrete time level m, Δt is the timestep size, and the γ_j are coefficients of an M-step Adams-Bashforth scheme. The $q_i^{*,m+1}$ are used to compute the ψ_i^{m+1} and ω_i^{m+1}. Corrected q_i^{m+1} are then computed from the ψ_i^{m+1} and ω_i^{m+1} via (24). The procedure is equivalent, except for errors associated with finite numerical precision, to a full solve for all fields, and hence the weak partial-slip boundary condition is correctly applied without the expense of a large coupled solve.

The model is implemented using the FEniCS system (Alnæs et al., 2009; 2014; Kirby, 2004; Kirby and Logg, 2006; Logg et al., 2012; Logg and Wells, 2010; Ølgaard and Wells, 2010) with the time discretisation optimised using the approach described in Maddison and Farrell (2014). The elliptic problem for the ψ_i^{m+1} is treated via projection onto discrete baroclinic modes, which leads to n decoupled elliptic problems. All linear systems are solved with LU decomposition using UMFPACK (Davis, 2004) via PETSc Balay et al. (2015a, 2015b, 1997).

Appendix C. Eddy buoyancy stress function

Consider a horizontal Helmholtz decomposition of the quasi-geostrophic eddy buoyancy fluxes in the form

$$\frac{f_0}{N_0^2}\overline{\mathbf{u}_g'b'}=-\nabla_H\chi_{eb}+\hat{\mathbf{z}}\times\nabla_H\xi_{eb}+\hat{\mathbf{z}}\times\boldsymbol{\Xi}_{eb}, \tag{C.1}$$

with $\nabla_H\cdot\boldsymbol{\Xi}_{eb}=(\hat{\mathbf{z}}\times\nabla_H)\cdot\boldsymbol{\Xi}_{eb}=0$. As for the eddy force function, the requirement that the elliptic problem for χ_{eb} defines a linear operator is imposed. The application of zero buoyancy boundary conditions, as per Bretherton (1966), combined with this linearity property, implies that $\chi_{eb}=0$ on the upper and lower surfaces.

It follows from (22) that in a simply connected domain the force function associated with the eddy buoyancy fluxes is given by

$$\nabla_H^2\Psi_{eb}=-\partial_z\nabla_H\cdot\left(\frac{f_0}{N_0^2}\overline{\mathbf{u}_g'b'}\right) \tag{C.2a}$$

$$\Psi_{eb}=0\ \text{ on }\ \partial\Omega. \tag{C.2b}$$

In particular:

$$\nabla_H^2\Psi_{eb}=\nabla_H^2\partial_z\chi_{eb}. \tag{C.3}$$

It is thus natural to define

$$\chi_{eb}=\int\Psi_{eb}dz \tag{C.4}$$

with $\chi_{eb}=0$ at the upper and lower surfaces. χ_{eb} is then a *stress* function, in the sense that the vertical derivative of the stress function yields a force function, whose horizontal curl yields an associated rotational momentum tendency.

For the multi-layer quasi-geostrophic equations this leads to

$$\chi_{eb,i+1/2}=-\sum_{j=1}^i H_j\Psi_{eb,j}$$
$$=\sum_{j=i+1}^n H_j\Psi_{eb,j}. \tag{C.5}$$

With this definition the left panel of Fig. (6) is equal to the negative eddy buoyancy stress function on the interface between the upper and middle layers, and the right panel of Fig. (6) is equal to the eddy buoyancy stress function on the interface between the middle and lower layers.

References

Alnæs, M.S., Logg, A., Mardal, K.-A., Skavhaug, O., Langtangen, H.P., 2009. Unified framework for finite element assembly. Int. J. Comput. Sci. Eng. 4 (4), 231–244.

Alnæs, M.S., Logg, A., Ølgaard, K.B., Rognes, M.E., Wells, G.N., 2014. Unified form language: a domain-specific language for weak formulations of partial differential equations. ACM Trans. Math. Softw. 40 (2), 9:1–9:37.

Andrews, D.G., McIntyre, M.E., 1976. Planetary waves in a horizontal and vertical shear: the generalized Eliassen-Palm relation and the mean zonal acceleration. J. Atmos. Sci. 33, 2031–2048.

Andrews, D.G., McIntyre, M.E., 1978. Generalized Eliassen-Palm and Charney-Drazin theorems for waves on axisymmetric mean flows in compressible atmospheres. J. Atmos. Sci. 35 (2), 175–185.

Bachman, S., Fox-Kemper, B., 2013. Eddy parameterization challenge suite I: Eady spin-down. Ocean Model. 64, 12–28.

Balay, S., Abhyankar, S., Adams, M.F., Brown, J., Brune, P., Buschelman, K., Dalcin, L., Eijkhout, V., Gropp, W.D., Kaushik, D., Knepley, M.G., McInnes, L.C., Rupp, K., Smith, B.F., Zampini, S., Zhang, H., 2015a. PETSc users manual. Argonne National Laboratory. ANL-95/11 - Revision 3.6

Balay, S., Abhyankar, S., Adams, M.F., Brown, J., Brune, P., Buschelman, K., Dalcin, L., Eijkhout, V., Gropp, W.D., Kaushik, D., Knepley, M.G., McInnes, L.C., Rupp, K., Smith, B.F., Zampini, S., Zhang, H., 2015b. PETSc web page. http://www.mcs.anl.gov/petsc.

Balay, S., Gropp, W.D., McInnes, L.C., Smith, B.F., 1997. Efficient management of parallelism in object oriented numerical software libraries. In: Arge, E., Bruaset, A.M., Langtangen, H.P. (Eds.), Modern Software Tools in Scientific Computing. Birkhäuser Press, pp. 163–202.

Barrett, K.E., 1978. A variational principle for the stream function-vorticity formulation of the Navier-Stokes equations incorporating no-slip conditions. J. Comput. Phys. 26 (2), 153–161.

Berloff, P., Hogg, A.M.C., Dewar, W., 2007. The turbulent oscillator: A mechanism of low-frequency variability of the wind-driven ocean gyres. J. Phys. Oceanogr. 37 (9), 2363–2386.

Bretherton, F.P., 1966. Critical layer instability in baroclinic flows. Q. J. R. Meteorol. Soc. 92 (393), 325–334.

Campion-Renson, A., Crochet, M.J., 1978. On the stream function-vorticity finite element solutions of Navier-Stokes equations. Int. J. Numer. Meth. Eng. 12 (12), 1809–1818.

Davis, T.A., 2004. Algorithm 832: UMFPACK V4.3 – an unsymmetric-pattern multifrontal method. ACM Tran. Math. Softw. 30 (2), 196–199.

Denaro, F.M., 2003. On the application of the Helmholtz–Hodge decomposition in projection methods for incompressible flows with general boundary conditions. Int. J. Numer. Meth. Fluids 43, 43–69.

Dritschel, D.G., McIntyre, M.E., 2008. Multiple jets as PV staircases: the Phillips effect and the resiliance of eddy-transport barriers. J. Atmos. Sci. 65 (3), 855–874.

Eden, C., 2010. Parameterising meso-scale eddy momentum fluxes based on potential vorticity mixing and a gauge term. Ocean Model. 32 (1–2), 58–71.

Eden, C., Greatbatch, R.J., Olbers, D., 2007. Interpreting eddy fluxes. J. Phys. Oceanogr. 37 (5), 1282–1296.

Fox-Kemper, B., Ferrari, R., Pedlosky, J., 2003. On the indeterminacy of rotational and divergent eddy fluxes. J. Phys. Oceanogr. 33 (2), 478–483.

Greatbatch, R.J., 2001. A framework for mesoscale eddy parameterization based on density-weighted averaging at fixed height. J. Phys. Oceanogr. 31 (9), 2797–2806.

Gresho, P.M., Sani, R.L., 2000. Incompressible flow and the finite element method. Isothermal laminar flow. John Wiley & Sons.

Griesel, A., Gille, S.T., Sprintall, J., McClean, J.L., Maltrud, M.E., 2009. Assessing eddy heat flux and its parameterization: A wavenumber perspective from a 1/10° ocean simulation. Ocean Model. 29 (4), 248–260.

Haidvogel, D.B., McWilliams, J.C., Gent, P.R., 1992. Boundary current separation in a quasigeostrophic, eddy-resolving ocean circulation model. J. Phys. Oceanogr. 22 (8), 882–902.

Harrison, D.E., 1978. On the diffusion parameterization of mesoscale eddy effects from a numerical ocean experiment. J. Phy. Oceanogr. 8 (5), 913–918.

Higham, N.J., 1993. The accuracy of floating point summation. SIAM J. Sci. Comput. 14 (4), 783–799.

Holland, W.R., Rhines, P.B., 1980. An example of eddy-induced ocean circulation. J. Phys. Oceanogr. 10 (7), 1010–1031.

Jayne, S.R., Marotzke, J., 2002. The oceanic eddy heat transport. J. Phys. Oceanogr. 32 (12), 3328–3345.

Kahan, W., 1965. Pracniques: further remarks on reducing truncation errors. Commun. ACM 8 (1), 40.

Karabasov, S.A., Berloff, P.S., Goloviznin, V.M., 2009. CABARET in the ocean gyres. Ocean Model. 30 (2–3), 155–168.

Kirby, R.C., 2004. Algorithm 839: FIAT, a new paradigm for computing finite element basis functions. ACM Trans. Math. Softw. 30 (4), 502–516.

Kirby, R.C., Logg, A., 2006. A compiler for variational forms. ACM Trans. Math. Softw. 32 (3), 417–444.

Lau, N.-C., Wallace, J.M., 1979. On the distribution of horizontal transports by transient eddies in the Northern Hemisphere wintertime circulation. J. Atmos. Sci. 36 (10), 1844–1861.

Logg, A., Mardal, K.-A., Wells, G.N. (Eds.), 2012. Automated Solution of Differential Equations by the Finite Element Method: The FEniCS Book. vol. 84 of *Lecture Notes in Computational Science and Engineering*. Springer.

Logg, A., Wells, G.N., 2010. DOLFIN: Automated finite element computing. ACM Trans. Math. Softw. 37 (2), 20:1–20:28.

Maddison, J.R., Farrell, P.E., 2014. Rapid development and adjoining of transient finite element models. Comput. Meth. Appl. Mech. Eng. 276, 95–121.

Maddison, J.R., Marshall, D.P., 2013. The Eliassen-Palm flux tensor. J. Fluid Mech. 729, 69–102.

Marshall, D.P., Maddison, J.R., Berloff, P.S., 2012. A framework for parameterizing eddy potential vorticity fluxes. J. Phys. Oceanogr. 42 (4), 539–557.

Marshall, D.P., Pillar, H.R., 2011. Momentum balance of the wind-driven and meridional overturning circulation. J. Phys. Oceanogr. 41 (5), 960–978.

Marshall, J., Shutts, G., 1981. A note on rotational and divergent eddy fluxes. J. Phys. Oceanogr. 11 (12), 1677–1680.

Marshall, J.C., 1984. Eddy-mean flow interaction in a barotropic ocean model. Q. J. R. Meteorol. Soc. 110 (465), 573–590.

McDougall, T.J., McIntosh, P.C., 1996. The temporal-residual-mean velocity. Part I: derivation and the scalar conservation equations. J. Phys. Oceanogr. 26 (12), 2653–2665.

McWilliams, J.C., 1977. A note on a consistent quasigeostrophic model in a multiply connected domain. Dyn. Atmos. Oceans 1 (5), 427–441.

Medvedev, A.S., Greatbatch, R.J., 2004. On advection and diffusion in the mesosphere and lower thermosphere: the role of rotational fluxes. J. Geophys. Res. 109 (D07104).

Nakamura, M., 1998. On modified rotational and divergent eddy fluxes and their application to blocking diagnoses. Q. J. R. Meteorol. Soc. 124 (545), 341–352.

Nakamura, M., Chao, Y., 2002. Diagnoses of an eddy-resolving Atlantic Ocean model simulation in the vicinity of the Gulf Stream. Part II: Eddy potential enstrophy and eddy potential vorticity fluxes. J. Phys. Oceanogr. 32 (6), 1599–1620.

Nurser, A.J.G., Lee, M.-M., 2004. Isopycnal averaging at constant height. Part II: Relating to the residual streamfunction in Eulerian space. J. Phys. Oceanogr. 34 (12), 2740–2755.

Ølgaard, K.B., Wells, G.N., 2010. Optimizations for quadrature representations of finite element tensors through automated code generation. ACM Trans. Math. Softw. 37 (1), 8:1–8:22.

Pedlosky, J., 1987. Geophysical Fluid Dynamics, second Springer-Verlag.

Plumb, R.A., 1986. Three-dimensional propagation of transient quasi-geostrophic eddies and its relationship with the eddy forcing of the time-mean flow. J. Atmos. Sci. 43 (16), 1657–1678.

Roberts, M.J., Marshall, D.P., 2000. On the validity of downgradient eddy closures in ocean models. J. Geophys. Res. 105 (C12), 28613–28627.

Taylor, G.I., 1915. Eddy motion in the atmosphere. Philosophical Trans. R. Soc. Lond. Ser. A, Contain. Pap. Math. Phys. Charact. 215, 1–26.

Vallis, G.K., 2006. Atmospheric and Oceanic Fluid Dynamics: Fundamentals and Large-Scale Circulation. Cambridge University Press.

Young, W.R., 2012. An exact thickness-weighted average formulation of the Boussinesq equations. J. Phys. Oceanogr. 42 (5), 692–707.